

ORIGINAL ARTICLE



A basal gradient of Wnt and stem-cell number influences regional tumour distribution in human and mouse intestinal tracts

Simon J Leedham,^{1,2} Pedro Rodenas-Cuadrado,¹ Kimberley Howarth,¹ Annabelle Lewis,¹ Sreelakshmi Mallappa,³ Stefania Segditsas,¹ Hayley Davis,¹ Rosemary Jeffery,⁴ Manuel Rodriguez-Justo,⁵ Satish Keshav,² Simon P L Travis,² Trevor A Graham,⁴ James East,² Susan Clark,³ Ian P M Tomlinson¹

► Additional materials are published online only. To view these files please visit the journal online (<http://dx.doi.org/10.1136/gutjnl-2011-301601>).

¹Molecular and Population Genetics, Wellcome Trust Centre for Human Genetics, University of Oxford, UK

²Translational Gastroenterology Unit, John Radcliffe Hospital, Oxford, UK

³Polyposis Registry, St Mark's Hospital, Harrow, UK

⁴Histopathology Laboratory, London Research Institute, London, UK

⁵Histopathology department, University College London Hospital, London, UK

Correspondence to
Dr Simon Leedham, Molecular and Population Genetics, Wellcome Trust Centre for Human Genetics, University of Oxford, Roosevelt Drive, OX3 7BN, UK;
simon.leedham@cancer.org.uk

Final note During the preparation of this manuscript Albuquerque *et al* published a paper screening human colorectal tumours for mutations in Wnt related genes and have independently proposed a similar mechanism to that suggested by us for the apparent non-random distribution of human colorectal tumours.²⁷

Accepted 15 December 2011
Published Online First
27 January 2012

ABSTRACT

Objective Wnt signalling is critical for normal intestinal development and homeostasis. Wnt dysregulation occurs in almost all human and murine intestinal tumours and an optimal but not excessive level of Wnt activation is considered favourable for tumorigenesis. The authors assessed effects of pan-intestinal Wnt activation on tissue homeostasis, taking into account underlying physiological Wnt activity and stem-cell number in each region of the bowel.

Design The authors generated mice that expressed temporally controlled, stabilised β-catenin along the crypt–villus axis throughout the intestines. Physiological Wnt target gene activity was assessed in different regions of normal mouse and human tissue. Human intestinal tumour mutation spectra were analysed.

Results In the mouse, β-catenin stabilisation resulted in a graduated neoplastic response, ranging from dysplastic transformation of the entire epithelium in the proximal small bowel to slightly enlarged crypts of non-dysplastic morphology in the colorectum. In contrast, stem and proliferating cell numbers were increased in all intestinal regions. In the normal mouse and human intestines, stem-cell and Wnt gradients were non-identical, but higher in the small bowel than large bowel in both species. There was also variation in the expression of some Wnt modulators. Human tumour analysis confirmed that different APC mutation spectra are selected in different regions of the bowel.

Conclusions There are variable gradients in stem-cell number, physiological Wnt activity and response to pathologically increased Wnt signalling along the crypt–villus axis and throughout the length of the intestinal tract. The authors propose that this variation influences regional mutation spectra, tumour susceptibility and lesion distribution in mice and humans.

INTRODUCTION

Wnt signalling plays a critical role in the development and homeostasis of the intestinal epithelium. Among other functions, the Wnt pathway is centrally involved in the maintenance of the stem-cell phenotype, control of epithelial cell localisation along the crypt–villus axis, secretory lineage development and the maturation of Paneth cells

Significance of this study

What is already known about this subject?

- Increased Wnt/β-catenin signalling underlies the initiation and progression of gastrointestinal tumours.
- An optimal but not excessive level of Wnt activation is considered favourable for tumorigenesis: the ‘just-right’ theory.
- There is marked variation in the distribution of murine and human intestinal tumours with a preponderance of small intestinal lesions in the mouse and colorectal tumours in the humans.
- Human tumour mutation spectra vary throughout the intestinal tract. For example, microsatellite unstable tumours are predominantly found on the right side of the colon.

What are the new findings?

- In a mouse model, stabilisation of β-catenin resulted in graduated neoplastic response down the length of the intestinal tract, with a marked increase in the number of stem and proliferating cells throughout.
- This graduated response mirrored underlying physiological gradients of stem cells, Wnt target gene activity and expression of some Wnt modulators throughout the intestines of *normal* mice.
- Similar but non-identical physiological gradients were found along *normal* human intestinal tracts and we have confirmed that human tumour APC mutation spectra are selected in different regions of the bowel.
- We propose that variation in stem-cell number and physiological Wnt activity influences regional mutation spectra, tumour susceptibility and lesion distribution.

(reviewed in Scoville *et al*).¹ The reliance of the intestinal epithelium on physiological Wnt signalling was demonstrated by Kuhnert *et al*² who demonstrated catastrophic loss of adult mouse

Significance of this study

How might it impact on clinical practice in the near future?

- This work improves our understanding of the mechanisms behind the non-random tumour distribution in human intestinal cancer.
- Targeted epithelial and mesenchymal manipulation of Wnt in colorectal cancers may prove to be an effective therapeutic strategy.

intestinal epithelial proliferation and crypt structure 7–10 days after adenoviral expression of the Wnt antagonist *Dickkopf-1*.

Wnt signalling is dysregulated in almost all intestinal neoplasia in the mouse and humans (reviewed by Radtke *et al*³). The adenomatous polyposis coli (APC) protein is a component of the canonical Wnt signalling pathway and is responsible for the regulation of the transcription factor β-catenin. Truncation or loss of APC disrupts the β-catenin degradation complex, increasing nuclear translocation of this transcription factor and causing increased expression of Wnt target genes (reviewed by Sieber *et al*⁴). Germline APC mutations are responsible for familial adenomatous polyposis (FAP), an autosomal dominant condition characterised by the formation of 100's to 1000's of colonic polyps. Most patients also develop adenomas of the duodenum, with many developing neoplastic gastric lesions (adenomas or fundic gland polyps) and the severity of colonic, gastric and duodenal polyposis varies within and among families. Somatic mutations in APC are also found in the majority of sporadic colonic adenomas⁵ and carcinomas.⁶

In human colorectal tumours, biallelic APC mutations occur non-randomly with respect to one another.⁷ Mutations are selected on their combined ability to produce an optimal, but not excessive, level of β-catenin activation in the tumour cell, a model subsequently dubbed the ‘just-right’ hypothesis.⁸ The majority of somatic APC mutations occur between codons 1250 and 1514, termed the mutation cluster region.^{6,9} This region of the gene encodes the first three of seven 20-amino acid β-catenin binding repeats (20AARs). Mutations in the mutation cluster region affect the numbers of 20AARs retained by the encoded protein and so alter its ability to bind and degrade β-catenin. In general, retention of a greater number of repeats results in more modest Wnt perturbation in the resultant polyp.

The number of 20AARs retained within a tumour varies according to the region of the intestinal tract in which the lesion is located. In FAP, germline mutations around codon 1300 are associated with copy-neutral loss of heterozygosity (LOH) and a very severe colonic phenotype. This mutation combination results in retention of one 20AAR per allele and is optimally selected in the rectal lesions of germline 1309 patients.¹⁰ Severe duodenal polyposis is associated with germline mutations after codon 1400, and somatic mutations that result in a cumulative total of four or more 20AARs in each upper gastrointestinal (GI) lesion are strongly selected.¹¹ Similar variability in mutation distribution is seen in sporadic colorectal tumours, with right-sided tumours retaining significantly more 20AARs than left-sided lesions.¹²

Analysis of the first hit/second hit relationship in human tissue is observational, based upon the site of APC mutations in established lesions. To further analyse the optimal level of Wnt signalling for tumourigenesis, *Apc*-mutant mice with different

numbers of retained 20AARs have been generated. We recently undertook a detailed molecular and phenotypic analysis of two *Apc*-mutant mice on the C57BL/6 background, *Apc*^{Min(R850X)} and *Apc*^{1322T13}.¹⁴ In tumours from both these animals the ‘second hit’ was LOH by mitotic recombination, resulting in cumulative 20AAR totals of 0 and 2, respectively. Polyp distribution was markedly different in these two strains: *Apc*^{1322T} animals developed a heavy tumour burden in the proximal small bowel (SB1) (segments 1 and 2) whereas *Apc*^{Min} mice had relatively more polyps in the distal small bowel (SB3) (segments 2 and 3).

Although there are differences between mice and humans, such as intestinal polyp location, the collated data show that an optimal level of Wnt signalling for GI tumourigenesis exists and that this level is submaximal. The evidence also demonstrates that cells of all types in the normal intestine require an optimal Wnt dosage, lower than in tumourigenesis, at different stages of their progression from stem cell—through progenitor, transit amplifying and differentiated phenotypes—to shedding into the gut lumen. We wished to assess how high-efficiency activation of Wnt signalling throughout the intestines would affect cell and tissue homeostasis, taking into account the underlying level of physiological Wnt signalling in each region of the bowel. We chose to study a transgenic mouse that expressed a temporally controlled, stabilised β-catenin protein. This mouse was preferred to *Apc*-mutant animals because β-catenin purely drives canonical Wnt signalling, preventing any hypothetical variation caused by non-LOH second hits at *Apc*, and avoiding the effects of losing non-Wnt functions of *Apc*.^{15,16} Here, we report the findings from this mouse and from our subsequent assessment of Wnt signalling in normal mouse and human intestines.

METHODS

Transgenic stabilised β-catenin mouse

Physiological degradation of the β-catenin protein occurs when GSK3β-mediated phosphorylation of serine/threonine residues signals for rapid ubiquitin-dependent proteosomal degradation. These serine/threonine residues are coded for by exon 3 of the gene. Harada *et al* generated a transgenic mouse with exon 3 flanked by loxP sites (*Ctnnb1*^{lox(ex3)/+}).¹⁷ Recombination with an intestinal driven Cre allowed transgenic in-frame deletion of the entire exon resulting in the expression of degradation resistant β-catenin.¹⁷ Subsequently, El Marjou *et al*¹⁸ demonstrated that a 9-kb regulatory region of the villin gene targeted stable and homogeneous expression of transgenes along the crypt-villus axis in the small and large intestines. We used this inducible Villin-cre system (*Villin-Cre*^{ERT2}) crossed with a *Ctnnb1*^{lox(ex3)/+} mouse on a C57BL/6 genetic background (gift of Mark Taketo) to allow temporal control over pan-intestinal epithelial β-catenin stabilisation in adult animals. Following Cre-mediated recombination, we denote the mice as *Ctnnb1*^{Δex3}. Genotyping and tissue collection are described in the online supplementary methods.

Assessment of colonic Cre-mediated recombination

In order to ensure that Cre recombination occurred uniformly and efficiently in the large intestine of the transgenic animals, we measured the amount of residual β-catenin exon 3 DNA using a standard absolute quantification method (online supplementary methods). Colonic epithelial tissue was laser dissected to minimise contamination from underlying normal stromal tissue and leucocytes. Normalised values for an epithelial cell population were expected to be close to 1 for control animals and 0.5 for heterozygous mice.

Laser capture microdissection and RNA extraction for stem-cell marker qRT-PCR

Six 5 µm serial sections were cut from the wild-type and transgenic colonic tissue blocks used for *in situ* hybridisation (ISH) and individual crypts were microdissected as previously described.¹⁹ RNA from individual crypts was extracted using Arcturus Paradise FFPE RNA isolation kit (Molecular Devices, Sunnyvale, California, USA) and underwent reverse transcription, amplification and quantitative reverse transcriptase PCR (qRT-PCR).

Immunohistochemistry

Immunohistochemistry for differentiated cell types, cell proliferation, apoptosis and β-catenin expression was completed using standard techniques (online supplementary methods and supplementary table 1).

Cell counting and statistical power

Crypt size, cell proliferation, stem-cell number, apoptotic cells and lineage marker expression were compared between a minimum of 100 crypts or crypt-villus units from each intestinal region, from a total of four *Ctnnb1Δex3* and wild-type littermates. Cells were counted by three different investigators (SL,

Figure 1 Stabilised β-catenin mouse dysplastic change in the small intestine parallels expansion of proliferating cells with abnormal β-catenin expression. In all intestinal regions there was expansion of the mid-crypt zone. In the proximal small bowel (SB1) this was so pronounced that it destroyed the crypt-villus architecture (Ai). The expanded mid-crypt cell population was dysplastic, actively proliferating (Ki-67 + immunostaining) (Aiii) and had abnormal expression of β-catenin (heavy nuclear or cytoplasmic) (Aii). Distal small bowel (SB3) to mid-small bowel (SB2) there was some preservation of normal cell morphology at the crypt bases and villi tips with Ki-67 negative cells (B, Ciii) and membranous β-catenin stain (B, Cii). The entire colon was morphologically non-dysplastic with membranous β-catenin staining (Dii); however, there was an expansion and upward shift of the Ki-67+ cells in comparison with wild-type controls (Dihi). Expansion of the stem-cell zone using S³⁵-UTP labelled *in situ* hybridisation for *Lgr5* (A-Eiv). There was expansion in the number of *Lgr5* expressing cells in all intestinal regions. In the *Ctnnb1Δex3* mouse colon the *Lgr5*+ cells were restricted to crypt bases but filled the bottom third of the phenotypically non-dysplastic crypt (Eiv), a considerable expansion of the stem-cell compartment in comparison with wild-type mouse colon (Eiv).

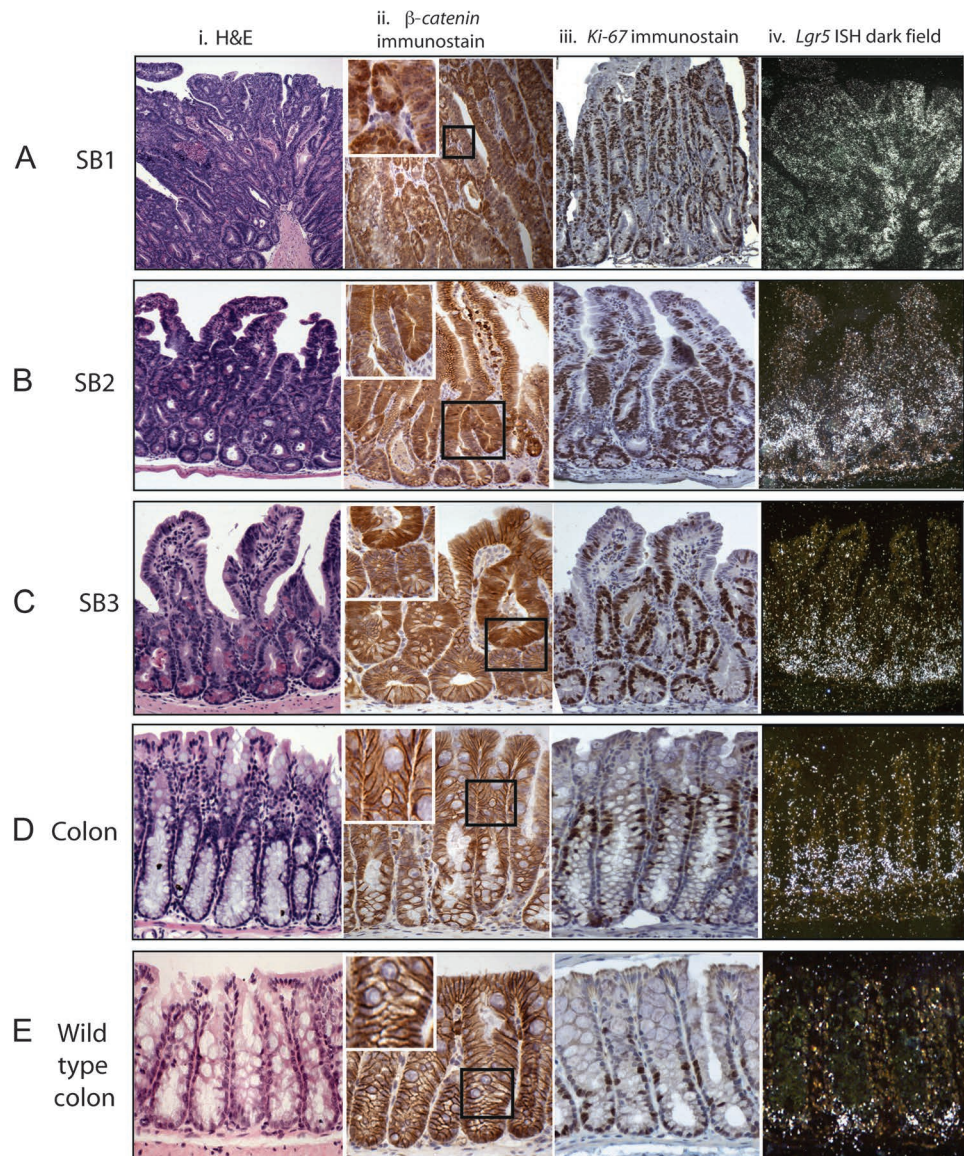
PRC, AL), blinded to the mouse genotype. The power to discern differences in cellularity between two intestinal compartments depends upon the magnitude of the difference between the compartments. By contrasting a minimum of 100 crypts from mutant animals to 100 crypts from wild-type animals we were able to detect effect sizes of approximately 0.7 with 99% power (assuming a t test was appropriate to compare between groups of n=100, and requiring a significance level of 0.01).

In situ hybridisation

Mouse model lineage tracing experiments have demonstrated that crypt based columnar cells specifically expressing *Leucine rich repeat containing G-protein coupled receptor 5 (Lgr5)* are capable of self-replication and multilineage differentiation in the intestine and colon.²⁰ mRNA ISH for *Lgr5* as a putative stem-cell marker was carried out on human duodenal, ileal and colonic biopsies from seven different patients and wild-type and transgenic mouse gut tissue as described in the online supplementary methods.

Normal mouse and human whole mount crypt analysis

Freshly dissected circles of wild-type mouse tissue from the SB1, mid-small bowel (SB2) and SB3, caecum and rectum were obtained using a 2 mm diameter punch biopsy tool. From the



human, biopsies of the duodenum, ileum, caecum and rectum were taken from upper and lower endoscopies performed on the same patient. Individual crypts were isolated by whole mount extraction and underwent RNA extraction and qRT-PCR for analysis of Wnt target gene expression (online supplementary methods). The remaining mesenchymal tissue after epithelial denudement was also isolated and processed.

Archival human sporadic and FAP associated polyps and tumours

Tissue collection

Upper GI biopsies and colectomy specimens from the same FAP patients and sporadic colorectal tumours with a clearly defined colonic location were obtained from pathology archives. Tissue sectioning, DNA extraction, APC sequencing and *5q* LOH analysis were completed as previously described¹⁹ (online supplementary methods).

Public mutation databases

The APC mutation status of additional sporadic colorectal tumours or cell lines was collected from the Catalogue of Somatic Mutations in Cancer (COSMIC v53 <http://www.sanger.ac.uk/genetics/CGP/cosmic/>) (online supplementary methods).

RESULTS

Pan-intestinal β -catenin stabilisation causes florid dysplasia in the small intestine but not in the colorectum

Four weeks after Cre induction, *Ctnnb1*^{Δex3} animals developed dysplastic changes in the GI tract. The proximal part of the small bowel was grossly thickened with a rubbery texture, but there were no discrete polyps produced either here or in any other part of the intestines. In the duodenum (SB1), microscopic analysis showed that the epithelium was carpeted by high-grade dysplastic cells, with complete destruction of crypt-villus architecture. The morphological appearance gradually improved distally. In the jejunum (SB2), high-grade dysplasia was only ubiquitous at the mid-crypt level. The crypts were greatly enlarged, but there was some preservation of architecture and normal cell morphology, especially at the tips of the villi and bases of the crypts. In the distal ileum (SB3), crypts were enlarged, with a variable mixture of mildly dysplastic and morphologically normal cells extending onto the villi (figure 1). The colon of the *Ctnnb1*^{Δex3} animals was macroscopically normal and microscopically non-dysplastic, but closer examination showed abnormalities. The colorectal crypts of *Ctnnb1*^{Δex3} animals were larger than those of their *Ctnnb1*-wild-type litter-mates, had significantly more cells ($p<0.0001$,

Table 1 Morphological and immunohistochemical findings from different intestinal regions of wild-type and *Ctnnb1*^{Δex3/+} mice

	Small bowel segment 1		Small bowel segment 2		Small bowel segment 3		Colon	
	WT	<i>Ctnnb1</i> ^{Δex3/+}	WT	<i>Ctnnb1</i> ^{Δex3/+}	WT	<i>Ctnnb1</i> ^{Δex3/+}	WT	<i>Ctnnb1</i> ^{Δex3/+}
Mean cell number/crypt (SEM)	35.3 (0.44)	Architecture destroyed	36.9 (0.39)	72.65 (1.36)	35.9 (0.4)	62.9 (1.14)	47.1 (0.48)	59.9 (0.7)
p Value	NA		<0.0001		<0.0001		<0.0001	
Mean Paneth cells/crypt-villus cells (per cent (SEM))	8.8/97 (9.1% (0.41))	11/153 (7.2% (0.45))	11.7/88 (13.3% (0.35))	16/169 (9.45% (0.22))	10.9/70 (15.53% (0.4))	11.1/85 (13.1% (0.33))	NA	NA
p Value	<0.0001		<0.0001		<0.0001		NA	
Mean entero-endocrine cells/crypt-villus cells (per cent (SEM))	0.9/95.1 (1% (0.26))	1.2/149 (0.9% (0.21))	1.1/89.5 (1.2% (0.26))	0.8/175.7 (0.5% (0.12))	0.8/70.4 (1.1% (0.17))	0.5/93.8 (0.5% (0.1))	0.9/53 (1.7% (0.31))	0.9/72 (1.2% (0.13))
p Value	0.2		0.02		0.05		0.1	
Mean goblet cells/crypt-villus cells (per cent (SEM))	7.1/95 (7.5% (0.37))	2.1/124.7 (1.7% (0.27))	6.1/89.5 (6.9% (0.41))	1.9/174.9 (1.1% (0.31))	7.4/67.7 (10.9% (0.7))	1.2/80 (1.5% (0.4))	13.5/54.6 (24.6% (1.9))	11.2/70.3 (16% (1.55))
p Value	<0.0001		<0.0001		<0.0001		=0.03	
Mean <i>Lgr5</i> + cells/crypt-villus cells (per cent (SEM))	4.1/94 (4.4% (0.4))	150/157.8 (99% (1.3))	3.4/92.5 (3.7% (0.23))	86/170.2 (50.5% (3.4))	2.1/69.3 (3% (0.45))	34.2/87 (39% (1.23))	0.8/50.1 (1.59% (0.3))	20.1/64 (31% (1.7))
p Value	<0.0001		<0.0001		<0.0001		<0.0001	
Mean Ki-67+ cells/crypt-villus cells (per cent (SEM))	19.2/98 (19.8% (1.16))	84.5/149 (56.71% (2.3))	23/89.7 (25.3% (1.23))	83/161 (52.6% (2.99))	19.9/66 (30% (1.32))	39/80 (48.7% (2.8))	14/52 (27% (1.34))	27/71 (38% (1.09))
p Value	<0.0001		<0.0001		<0.0001		<0.0001	
Mean number cleaved caspase 3+ cells/1000 nuclei (SEM)	0.6 (0.04)	26.5 (1.1)	0.7 (0.1)	7.3 (1.3)	0.8 (0.1)	5.3 (0.7)	1.1 (0.1)	5.5 (0.3)
p Value	0.002		0.002		0.002		0.002	
Mean crypts in fission/colon (SEM)	NA	NA	NA	NA	NA	NA	0.25 (0.25)	26 (4.2)
p Value	NA		NA		NA		0.03	
β -Catenin immunostain	Membranous	Heavy nuclear/cytoplasmic	Membranous	Membranous on villi tips and crypt bases. Heavy cytoplasmic elsewhere	Membranous	Cytoplasmic staining in mid-crypt dysplastic areas. Membranous elsewhere	Membranous	Membranous

The table shows the mean number and percentage of cells per tissue unit on well-orientated cross-sections. A minimum of 50 crypts/crypt-villus units were counted from four different mutant mice. The number of crypts in obvious fission were counted in entire colon rolls from four wild-type and four mutant mice. p Values were calculated using Mann–Whitney U test (Prism, Graphpad Software, La Jolla, California, USA).

WT, wild-type.

Mann–Whitney U test) and had a higher prevalence of fission ($p=0.03$, Mann–Whitney U test) (table 1).

All differentiated cell types were present in dysplastic tissue (table 1). Although there was an absolute increase in small intestinal Paneth cell numbers in transgenic tissue, the increase in crypt size led to transgenic crypts having proportionally fewer of these cells than their wild-type counterparts ($p<0.0001$, Mann–Whitney U test). Paneth cells were also displaced from the base in mutant crypts (online supplementary figure 1).

Immunohistochemistry showed β -catenin expression in *Ctnnb1^{Δex3}* mice to parallel dysplasia throughout the intestine. In SB1, β -catenin was predominantly heavily nuclear with some regions of cytoplasmic staining. In SB2 and SB3, expression was cytoplasmic in the dysplastic cells in the mid-crypt zone and predominantly membranous otherwise, including at the preserved villus tips in the SB2 to SB3. Membranous β -catenin staining was seen in all morphologically non-dysplastic epithelial cells, including the entire large bowel of *Ctnnb1^{Δex3}* mice and throughout the intestines of control animals (table 1, figure 1).

Cell proliferation marker expression in the *Ctnnb1^{Δex3}* mice correlated strongly with dysplasia and β -catenin expression. Where crypt-villus architecture was maintained, the proliferative zone filled the dysplastic mid-crypt region. It was significantly enlarged ($p<0.0001$, Mann Whitney test) and shifted towards the tops of the crypts in comparison with control mice

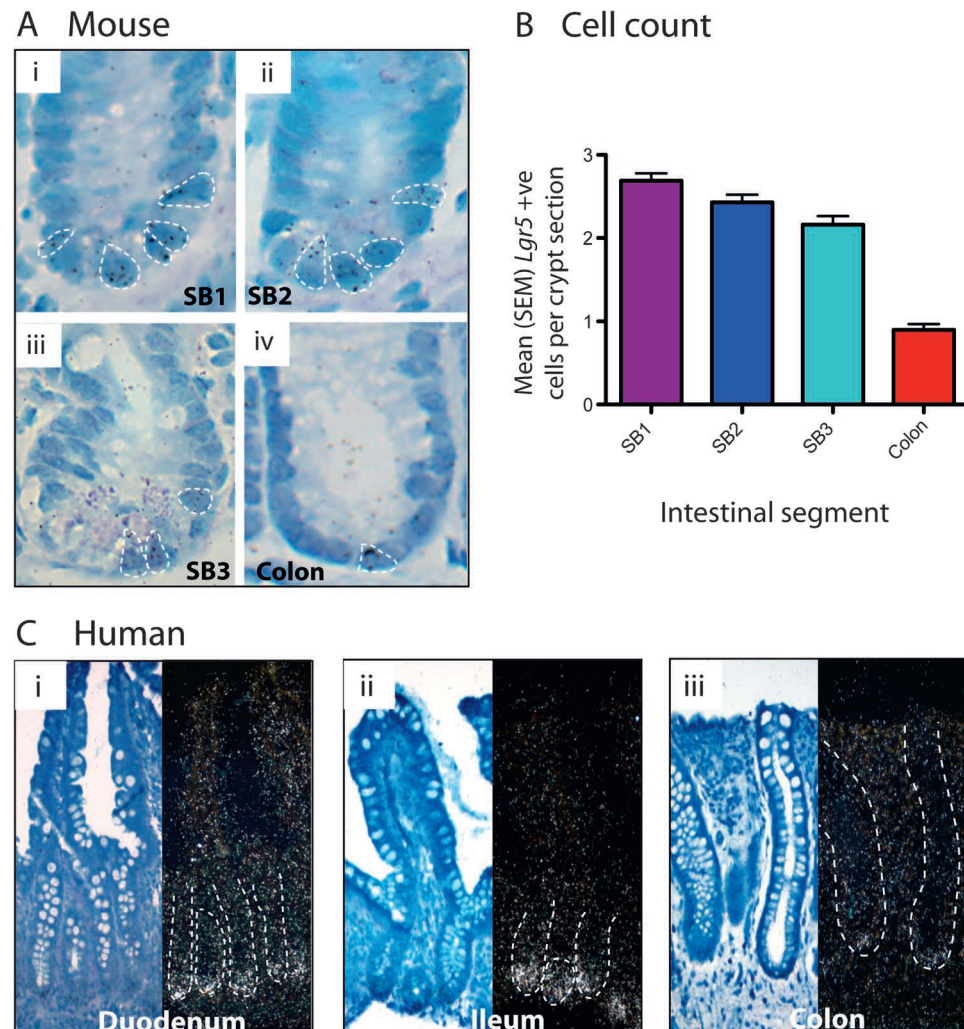
(table 1, figure 1). Apoptosis, as determined by cleaved caspase 3 immunohistochemistry, was increased in all dysplastic tissue ($p=0.002$) (online supplementary figure 1).

In order to show that the absence of colorectal neoplasia in the colon of transgenic mice was not simply the result of lack of Cre expression and/or recombination in the large intestine, we measured the amount of residual wild-type β -catenin in laser-dissected colonic epithelium from *Ctnnb1^{Δex3}* mice compared with their wild-type litter-mates. The mean dosage of wild-type β -catenin was 0.49 (SEM 0.02) in *Ctnnb1^{Δex3}* mice relative to the wild-type animals (mean 1.1 (SEM 0.03)), showing very high efficiency recombination and demonstrating that the non-dysplastic colonic phenotype was not simply a consequence of variable intestinal Cre activity.

Stem-cell marker expression in *Ctnnb1^{Δex3}* mice

We next assessed the expression of established stem-cell markers in the *Ctnnb1^{Δex3}* mice compared with wild-type animals. ISH demonstrated a huge expansion in the *Lgr5*-expressing cell population throughout the small intestine. The most pronounced changes were in SB1, where the entire epithelium was *Lgr5*+. In SB2 and SB3, *Lgr5*+ cells were predominantly basal, as in normal tissue, although the stem-cell zone was expanded, extending into the mid-crypt region and overlapping with the mid-crypt proliferative/dysplastic zone (figure 1).

Figure 2 Stem-cell numbers vary through the intestinal tract. (A) Mouse *in situ* hybridisation (ISH). H3-UTP labelled ISH for *Lgr5* on well-orientated crypts from a wild-type mouse: (i) proximal small bowel (SB1); (ii) mid-small bowel (SB2); (iii) distal small bowel (SB3); and (iv) colon. Individual cells containing ≥ 4 silver granules were counted and are highlighted in each picture. (B) Mouse *Lgr5*+ cell counts. Mean (SEM) *Lgr5*+ cell counts are shown. *Lgr5*+ cells are maximal in the SB1 with a slightly reducing number through to the ileum (SB3). A profound drop in *Lgr5*+ cells is seen in the colon ($p<0.001$, analysis of variance). Cell numbers were counted in 100 crypts from each region from three different wild-type mice. (C) Human ISH. S³⁵-UTP labelled ISH for *LGR5* on human endoscopic biopsy specimens from: (i) duodenum (ii) ileum and (iii) colon of the same patient. *LGR5* expression was restricted to the crypt bases and was maximal in the ileum, with only single *LGR5*+ cells seen in colonic crypts. ISH was carried out on biopsy sections from 7 different patients undergoing normal upper and lower endoscopies.



Colon

In the large bowel, despite normal morphology, *Lgr5*+ cells filled the bottom third of the crypt, representing a considerable expansion of the putative stem-cell population in comparison with wild-type controls (figure 1D,E). qRT-PCR on a total of 45 individual laser-microdissected crypts confirmed higher expres-

sion of *Lgr5* in the large bowel of *Ctnnb1^{Δex3}* animals, with a mean 9.2-fold increase (SEM 1.3; p=0.002, t test) compared with wild-type litter-mates. Another colonic stem-cell marker, *Ascl2*, was also more highly expressed in the mutant animals (mean increase 9.3-fold, SEM 2.3; p=0.02, t test).

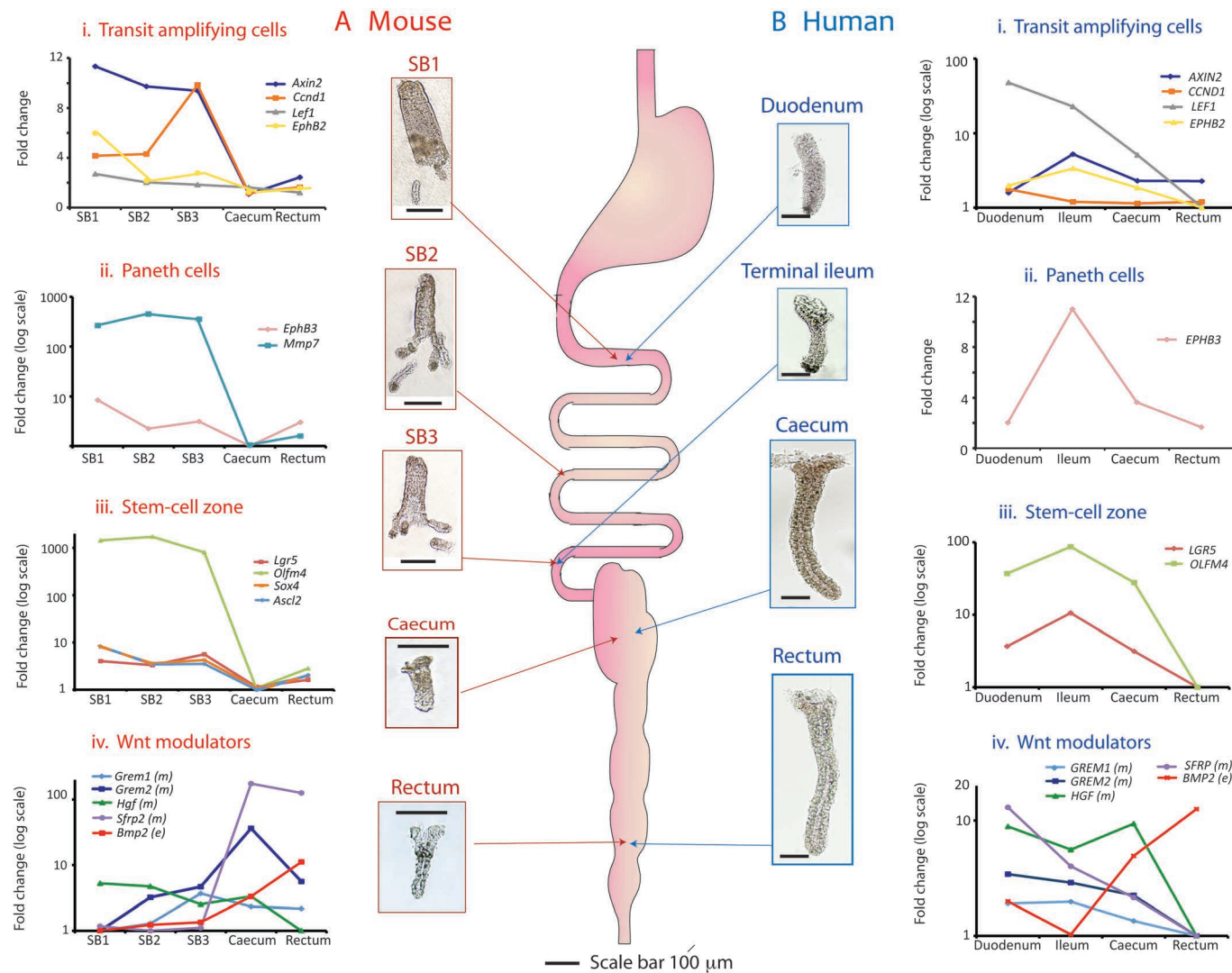


Figure 3 Individual crypt Wnt target gene expression varies longitudinally throughout the normal mouse and human intestinal tract. Thumb nail pictures show whole mount intestinal crypts and villi from the different regions of normal mouse and human intestine after EDTA extraction. Mouse villi are pictured purely to provide scale; in fact, only individual crypts were aspirated and used in analysis. Mesenchymal tissue was isolated after complete epithelial denudement. Scale bar 100 µm. Five crypts were dissected from each intestinal region, analysed individually and used to calculate a mean ΔCt, which was then averaged across three wild-type mice (online supplementary table 2A) and four human patients (online supplementary table 2B). Mean ΔΔCt values were used to calculate expression fold changes compared with the region of minimal expression. (A) Mouse gene expression category 1 Wnt target genes (transit amplifying cells) showed quite variable expression along the intestine but were maximally expressed in the proximal small bowel (SB1) (with the exception of *Cyclin D1*). Category 2 genes (Paneth cells) were expressed in the small intestine as expected from this cell distribution (p<0.001, analysis of variance (ANOVA)). Category 3 genes (stem-cell zone) showed very similar expression profiles with maximal expression in the small intestine declining markedly in the colon with minimal expression seen in the caecum (p<0.001, ANOVA). *Sax4* expression closely mirrored that of *Ascl2* and a striped line indicates the regions of identical expression. Conversely, epithelial *Bmp2* expression was minimal in the duodenum climbing steadily to a peak in the mouse rectum (p<0.001, ANOVA), and there was also significant variability in the expression of some of the mesenchymal Wnt modulators (*Grem2* and *Hgf*, p<0.05, ANOVA). The expression of the mesenchymal Wnt antagonist, *Sfrp2*, varied considerably with colonic expression more than 130-fold greater than that in the small intestine (p=0.035, ANOVA). (B) Human gene expression. All human Wnt target genes were maximally expressed in the ileum and minimally expressed in the rectum with the exception of the category 1 genes *LEF1* and *CYCLIN D1 (CCND1)*, which were maximally expressed more proximally. Category 3 (stem-cell) gene expression peaked in the ileum correlating with the human in situ findings (p<0.001, ANOVA). Caecal stem-cell marker expression is significantly greater than that seen in the rectum. The inverse correlation was seen for epithelial *BMP2* expression (p<0.001, ANOVA). Expression of the mesenchymal Wnt modulators was generally higher in the human small intestine which contrasted sharply with the murine *Gremlin 1, 2* and *Sfrp2* expression gradients. Only the expression gradient for *HGF* reached statistical significance in the humans (p=0.05, ANOVA) as the result of a 10-fold difference in expression from the caecum to the rectum. SB1, proximal small bowel; SB2, mid-small bowel; SB3, distal small bowel.

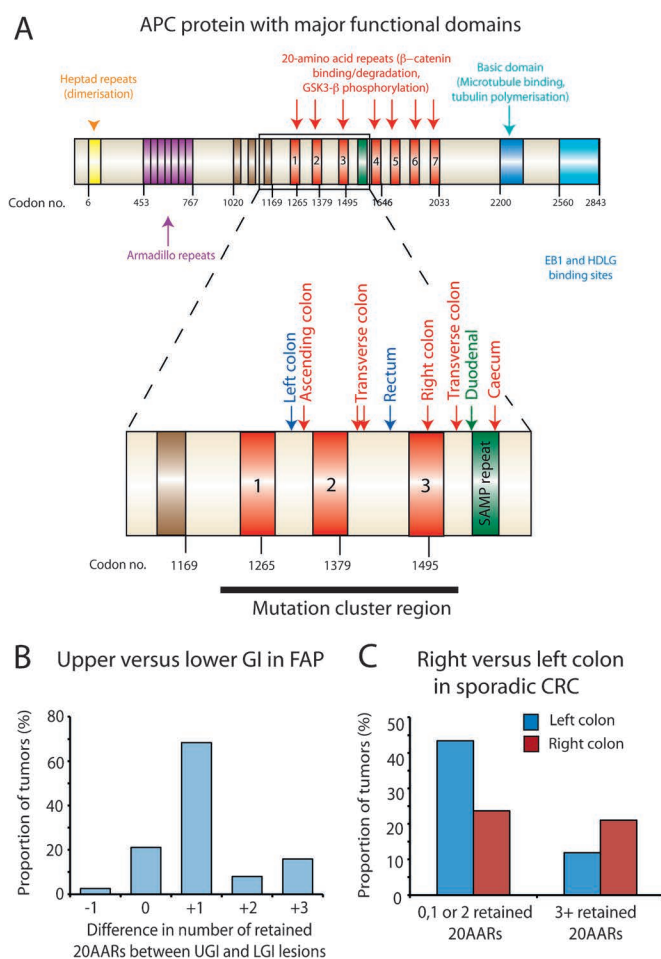


Figure 4 The adenomatous polyposis coli (APC) mutation spectrum varies with intestinal region in familial adenomatous polyposis (FAP) and sporadic gastrointestinal tumours. (A) Mutation spectra of upper and lower gastrointestinal (GI) lesions taken from the same FAP patient. The major functional domains of the APC protein are shown with an enlargement of the mutation cluster region. The number of retained 20-amino acid β -catenin binding repeats (20AARs) was calculated in upper GI (UGI) and lower GI (LGI) lesions taken from the same individual FAP patient(s) after determination of the mutation spectra of each lesion. The mutations for one individual patient (patient 1, online supplementary table 3) are mapped out (UGI lesion, green; right colon, red; left colon, blue). (B) UGI lesions in FAP retain significantly more 20AARs than LGI lesions taken from the same patient. The number of retained repeats from LGI lesions was subtracted from the number of repeats retained in the same patients' UGI lesions and the difference plotted. Significantly more repeats were retained in UGI lesions resulting in a more modest Wnt perturbation in these lesions ($p<0.001$, binomial test). (C) Right sided sporadic colorectal cancers and cell lines retain significantly more 20AARs than left sided lesions. Lesions in our sporadic data set of 76 tumours (online supplementary table 4A and B) were categorised by their distribution and the cumulative number of retained 20AARs after identification of first and second hits at APC in all lesions. Tumours retaining a cumulative total of three or more 20AARs were more likely to arise proximally whereas on the left side of the colon, mutations that retain fewer 20AARs were optimally selected to produce a greater Wnt perturbation in the resultant polyp ($p=0.03$, Fishers Exact test).

Stem-cell marker and Wnt target gene expression gradients are present in normal mouse intestine

Our mouse model showed considerable phenotypic variation along the intestinal tract in response to pan-intestinal Wnt perturbation. We hypothesised that this might, in part, reflect

underlying physiological gradients and so we also investigated the cephalo-caudal stem-cell and Wnt signalling gradients in the GI tract of wild-type litter-mates.

First, we used high-resolution 3 H-UTP in situ assessment of mRNA for the stem-cell marker *Lgr5* on well-orientated crypts (figure 2A) to allow accurate counting of the number of cells expressing stem-cell markers in the different intestinal regions. *Lgr5* ISH showed a gradually decreasing stem-cell number progressing from SB1 to SB3, but then a marked reduction in the large bowel (ANOVA $p\leq 0.001$) (figure 2B).

Next, we identified robust Wnt target genes based on consistent changes in a combination of experiments (details not shown): lithium chloride inhibition of GSK3 β ²¹ in the normal RIE-1 intestinal cell line (Leedham, unpublished data, 2010) and exon mRNA expression microarray and qRT-PCR in tumours from *Apc*-mutant mice.¹³ Wnt target genes were chosen and subdivided into the categories defined by Van der Flier *et al*:²²

1. genes expressed in the rapidly dividing transit amplifying cells (*Axin2*, *EphB2*, *CyclinD1*, *Lef1*)
2. genes expressed by post-mitotic Paneth cells (*EphB3*, *Mmp7* (mouse only))
3. genes expressed in the stem-cell position of the crypt (*Lgr5*, *Olfm4* and *Ascl2* (mouse only), *Sox4* (mouse only)).

We then used qRT-PCR assays of identified Wnt target gene mRNA in order to measure overall expression levels in individual crypts taken from different regions of the mouse intestine (figure 3A and online supplementary table 2A). Wnt target gene expression varied considerably down the length of the intestinal tract (figure 3A), with expression in the small bowel greater than that in the colon, correlating with the *Lgr5* ISH findings. Minimal Wnt target expression was seen in the caecum.

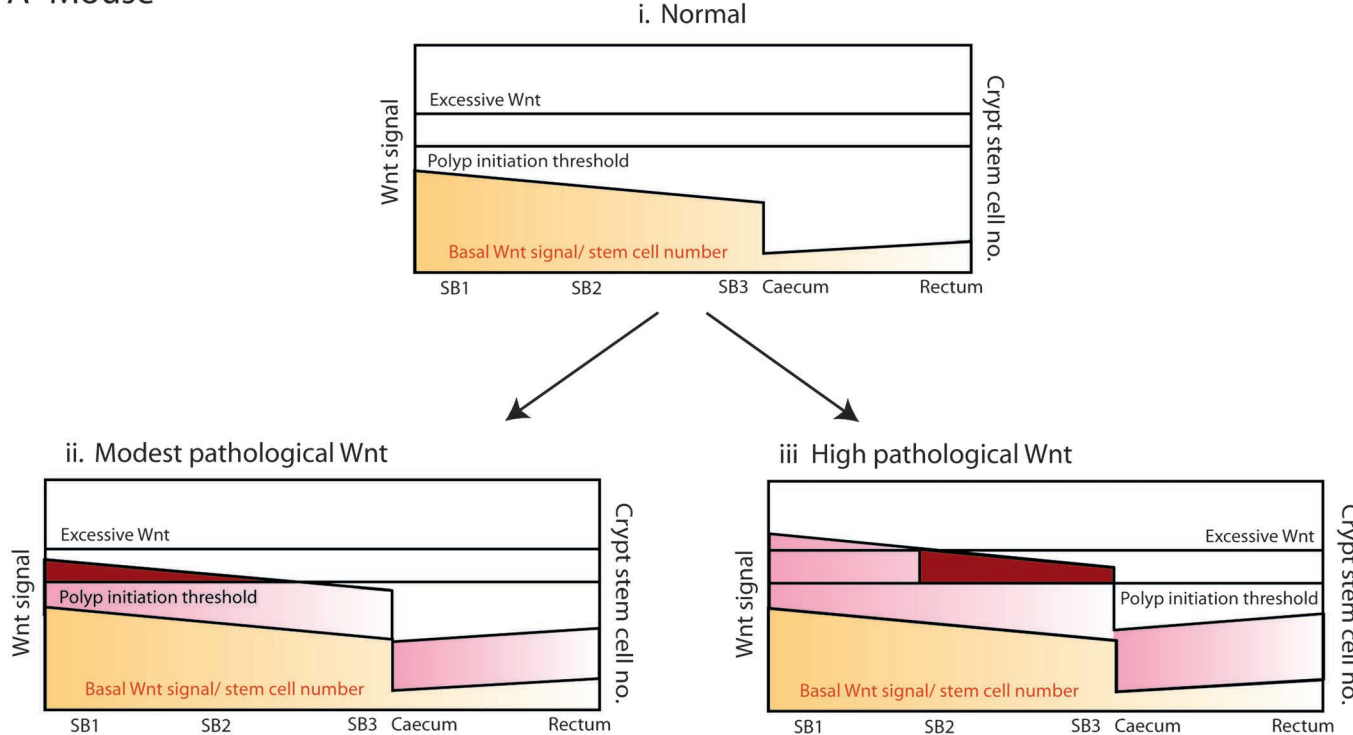
We also demonstrated variability in the regional expression of some established epithelial and mesenchymal Wnt modulators (figure 3A and online supplementary table 2A). There was a considerable gradient in expression of the Wnt antagonist *Sfrp2* in the mouse, with mesenchymal expression in the colon more than 130-fold greater than that in the small intestine. *Sfrp2* is a potent inhibitor of endogenous Wnt activity in rat normal intestinal epithelial cells (online supplementary results, online supplementary figure 2), and so its high expression is likely to contribute to the low epithelial Wnt activity in the mouse large bowel. *Dickkopf 1, 2, 3* and *R-spondin 1, 2, 3* expression were also measured but no appreciable intestinal gradient detected (data not shown).

Human tumour mutation spectra and wnt gradient in the normal human intestines

In *Ctnnb1*^{Δex3} mice, the distribution of dysplasia paralleled the physiological Wnt and stem-cell gradient. β -Catenin mutations are, however, rare in human bowel tumours which usually dysregulate Wnt through APC mutations. These mutations are under selective constraints such that stem cells acquire an optimal but not excessive level of Wnt signalling.^{7,8} Existing data from different FAP patients support the existence of different APC mutation spectra in tumours from different locations in the bowel.^{10,12,23} In order to compare the somatic mutation profiles of upper and lower GI tumours from the same patient, we studied a new set of FAP patients from whom gastric/duodenal and colonic lesions had been sampled. This allowed us to control for the effects of variation among patients and potential confounding factors such as diet. We demonstrated that upper GI lesions in FAP retain significantly more 20AARs than lower GI lesions taken from the same patient (figure 4 and online supplementary table 3).

Colon

A Mouse



B Human

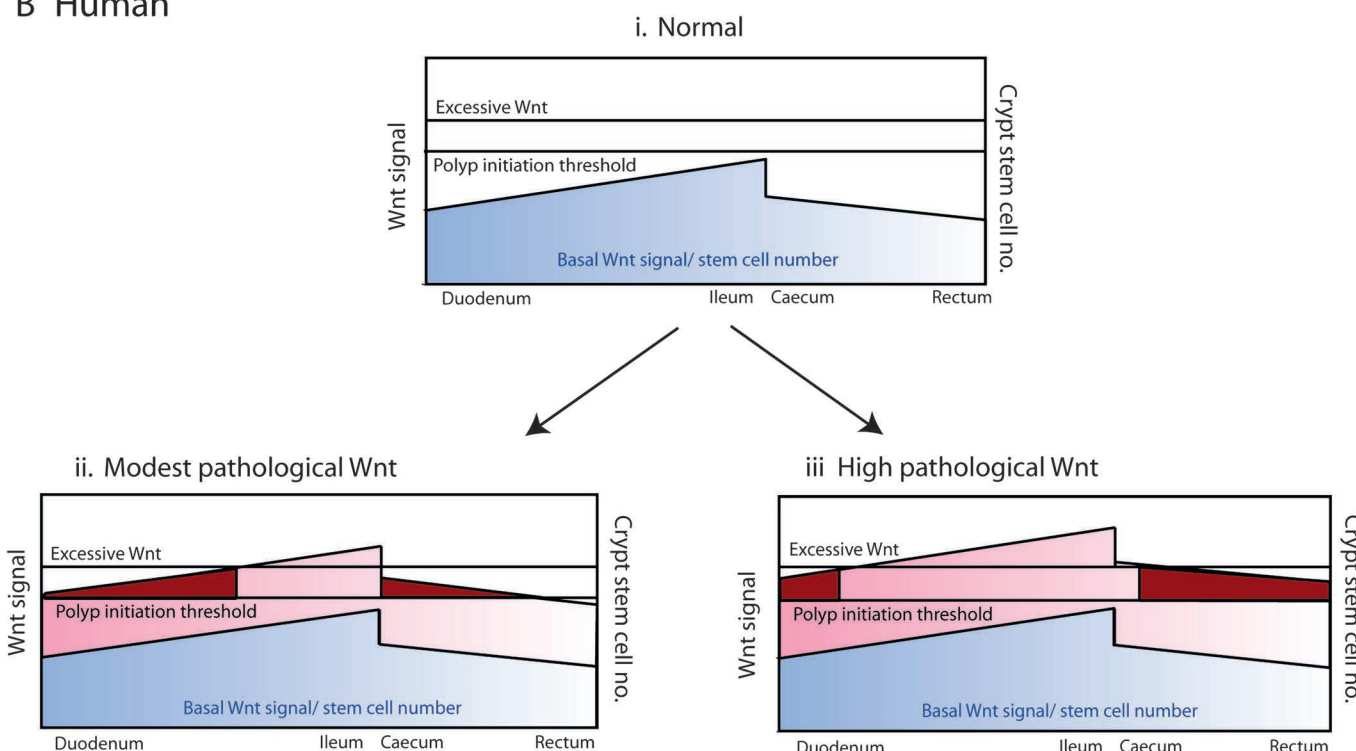


Figure 5 ‘Just-right’ theory and genotype–phenotype correlations. (Ai and Bi) Basal Wnt signalling and stem-cell number in the mouse and humans. Mouse and human basal Wnt target expression profile and stem-cell number vary down the length of intestinal tract (figure 3). The two species have quite distinct profiles which in combination with ‘just-right’ mutation spectra may contribute to intestinal lesion distribution. (Aii and Aiii) The consequences of pathological Wnt signalling in the mouse. Submaximal pathological Wnt perturbation (seen in *Ctnnb1*^{Δex3} and *Apc*^{1322T} mice, as evidenced by low levels of nuclear β-catenin expression¹⁴) breaches the dysplasia threshold in the proximal small intestine where basal Wnt expression and stem-cell numbers are the highest, resulting in a heavy proximal small bowel (SB1) and mid-small bowel (SB2) lesion burden. In the mouse colon, the Wnt perturbation is insufficient to cause dysplasia in the colon despite causing an increase in the stem-cell number. Maximal Wnt perturbation as seen in the *Apc*^{Min(R850X)} is excessive and thus suboptimal proximally; hence, a predominantly distal small bowel (SB3) polyp distribution is characteristic. Maximal lesion distribution shown with dark red shading. (Bii and Biii) The consequences of pathological Wnt signalling in the humans. Modest Wnt perturbations such as that resulting from mutations that retain several 20-amino acid β-catenin binding repeats (20AARs)

Next, we genotyped and examined the mutation spectra of 19 sporadic colorectal cancers with known colonic distribution. This was combined with the data from 57 other sporadic tumours and cell lines taken from COSMIC v53. We only included lesions where we could identify both somatic hits at *APC* to give an accurate measure of the number of retained 20AARs (online supplementary table 4A,B). Right-sided lesions (transverse, ascending colon and caecum) had a higher frequency of mutations that retained a total of three or more 20AARs than left-sided colonic lesions (descending colon, sigmoid and rectum) (χ^2 test, $p=0.03$). These data validate and add to the work by Albuquerque *et al*¹² demonstrating that the optimal tumourigenic level of Wnt signal varies within the different regions of the colon in sporadic tumours as well as between the colon and small intestine in FAP (figure 4, online supplementary tables 3 and 4).

To our knowledge, physiological stem-cell and Wnt gradients have not previously been investigated in the *normal* human intestine. Based on our findings in the mouse we hypothesised that such gradients might contribute to established human tumour selective constraints. First, we assessed *LGR5* mRNA expression in normal intestinal biopsy tissue taken from the duodenum, ileum and colon of the same patients. In contrast to the mouse, maximal stem-cell marker mRNA expression was seen in the ileum in humans (figure 2C).

Next, human Wnt target genes were chosen and categorised as for the mouse and their expression levels assayed in isolated crypts by qRT-PCR. Similar to the mouse, normal human Wnt target gene expression showed considerable variability down the length of the intestinal tract (figure 3B and online supplementary table 2B). However, the majority of genes were maximally expressed in the ileum, consistent with the human *LGR5* ISH results. Epithelial *BMP2* and mesenchymal *BMP* antagonist expression was consistent with the observed stem-cell gradient. Mesenchymal HGF expression varied 10-fold between the caecum and rectum. As this is a potent morphogen that promotes nuclear β -catenin translocation in human CRC cells,²⁴ this gradient may contribute to the observed difference in epithelial Wnt target gene activity between the human caecum and rectum. *Dickkoff 1, 2, 3* and *R-spondin 1, 2, 3* expression was also measured but no appreciable intestinal gradient was detected (data not shown).

DISCUSSION

Intestinal cell fate is determined by morphogen concentration gradients, mediated by complex interactions between an array of signalling molecules, receptors and antagonists. The importance of the Wnt pathway in the control of cell proliferation and the maintenance of intestinal stem cells is well established. Here, we have demonstrated variable stem-cell number and physiological Wnt pathway activity in different regions of the normal murine and human intestinal tracts.

Using a mouse model, we have also shown a graduated response to β -catenin stabilisation. All regions of the intestines showed an expansion of two overlapping populations of cells: (1) stem cells, predominantly at the crypt base and (2) prolif-

erating, dysplastic cells, usually at the mid-crypt zone. The most profound changes were in SB1, where the entire epithelium was disordered and filled with stem-like, proliferating cells. In the large bowel, this stem and proliferating cell expansion was coupled with an increase in the crypt size and rate of fission, but normal architecture was largely retained and there was no dysplasia. As *Villin-CreERT2* drives Cre-mediated recombination homogeneously throughout the crypt-villus axis and along the intestines,¹⁸ these data suggest an inherently variable response to increased Wnt signalling. Kuhnert *et al*² showed that the effect of systemically antagonising Wnt by *Dickkopf-1* expression similarly varied down the length of the murine intestine with the most profound effect in SB1. We demonstrated that this intrinsic sensitivity to Wnt modulation along the caudal-cephalic axis of the intestine mirrored the physiological gradient expression of the stem-cell markers *Lgr5* and *Olfm4*. Recent work has shown that the stem-cell marker *Lgr5* functions as a Wnt receptor component that mediates Wnt signal enhancement via soluble R-spondin protein.²⁵ As a Wnt signalling enhancer and target gene, *Lgr5* appears to be subject to positive auto-regulation corroborated by the marked expansion of the *Lgr5* expressing cell population following β -catenin stabilisation here, and in response to the wnt agonist R-spondin.²⁶ As physiological *R-spondin* expression was consistent throughout the intestine we hypothesise that an intestinal gradient of *Lgr5* expression may influence this regional inherent sensitivity to Wnt signalling and the response to pathological Wnt excess.

An intriguing question is whether the differences in dysplasia along the intestines of the *Ctnnb1Δex3* mouse are related to our previous observations⁷—confirmed in this manuscript—that specific *APC* mutation spectra are optimally selected in different regions of the human bowel. These observations, dubbed the ‘just-right’ model,⁸ propose that a threshold of Wnt signalling needs to be reached for dysplastic lesions to form, but that the optimum Wnt level for tumourigenesis is submaximal. Our mouse and human data provide clues to suggest that one reason for different *APC* mutations in tumours along the GI tract is a different physiological level of Wnt and stem-cell number. Hence, for example, when a modest pathological Wnt perturbation is superimposed on a low level of physiological Wnt—as in the colon of *Ctnnb1Δex3* mice—the resultant Wnt level is still too low to cause dysplasia (figure 5A). In humans, the caecum has higher Wnt levels than the rectum, consistent with the selection of mutant *APC* alleles that retain a greater number of 20AARs. In microsatellite unstable cancers, this selection is favoured by the presence of multiple mononucleotide and dinucleotide repeats between codons 1450 and 1560 of *APC* that are prone to slippage in mismatch repair deficiency. Along with Albuquerque *et al*^{12, 27} we speculate that it is this retention of 20AARs in mismatch repair deficient tumours that accounts for the right-sided colonic distribution of these tumour types.

Homeostatic Wnt signalling and stem-cell numbers in the normal intestine are subject to auto-regulatory and combinatorial control with a complex network of interacting mesenchymal and epithelial morphogenetic pathways.²⁸ We have demonstrated intestinal gradients of some important Wnt and

[Continued]

favour lesion development in the upper gastrointestinal (GI) and right colonic regions, explaining the more severe upper GI phenotype seen in patients with germline mutations after codon 1400. Conversely, early mutation cluster region mutations retain fewer 20AARs resulting in a greater degree of Wnt perturbation. Excessive Wnt is suboptimal for upper GI lesions but favours more distal lesions resulting in a severe colonic phenotype with loss of heterozygosity optimally selected in the rectum of patients with germline codon 1309 mutations.¹⁰ Maximal lesion distribution is shown with dark red shading.

stem-cell modulators such as *Bmp2*, *Gremlin 1, 2* and *Hgf* in the epithelium and mesenchyme of humans and mice. Variable mesenchymal-epithelial cross talk along the intestinal tract is likely to influence physiological epithelial Wnt activity. In particular, the marked *Sfrp2* expression gradient between the mouse colon and small intestine may contribute to the very low level of physiological epithelial Wnt activity seen in the murine colon, as we have shown that *Sfrp2* is a potent and dose-dependent antagonist of endogenous Wnt activity (online supplementary figure 2). As this gradient in the mouse is the reverse of that seen in the humans (online supplementary figure 2), we hypothesise that the antagonism of Wnt activity by factors such as *Sfrp2* in the mouse colon may contribute to the differential intestinal polyp distribution in humans and mice. Interestingly, van Veelen *et al* have recently shown that coactivating intestinal Wnt signalling by *Apc* deletion and by a mechanism mimicking receptor tyrosine kinase phosphorylation of β-catenin markedly shifted murine intestinal tumour distribution towards the colon.²⁹ This suggests that the maintenance of low physiological Wnt activity in the mouse colon by ligand sequestering antagonists such as *Sfrp2* may be partly counteracted by pathological activation of Wnt via an alternative (Wnt ligand and Frizzled receptor independent) mechanism, resulting in sufficient Wnt activity to breach the colonic Wnt signalling threshold and initiate colonic tumour formation. Regional variation in tyrosine kinase receptor expression has been reported in the normal human colon with epidermal growth factor receptor expression significantly higher proximally,³⁰ correlating with the higher physiological Wnt activity we have demonstrated in the human right colon. Furthermore, variation in the pattern of epigenetic change has also been reported in the normal human large intestine.³¹ Methylation and transcriptional silencing of Wnt signalling genes have been shown to occur in morphologically normal crypts,³² and are common in colorectal tumours.³³ Physiological regional variation in epigenetic transcriptional silencing or non-canonical Wnt activation may contribute to the marked variability in Wnt target gene activity demonstrated here.

We have generated a simple model in an attempt to explain multiple genetic events and complex physiological pathways and recognise the limitations of attempting to do this. There are a number of phenomena that this model cannot explain such as the disparity in prevalence between sporadic duodenal and caecal lesions in humans despite similar basal Wnt and stem-cell numbers in these two regions. While these data support the influence of Wnt signalling and stem-cell number variation on tumour distribution, there are also a number of potential confounding factors that have not been assessed such as the effect of intraluminal toxins and the contribution of the intestinal flora.

We propose that variable gradients in physiological Wnt activity and stem-cell number influence Wnt responsiveness along the crypt-villus and caudal-cephalic axes of the intestinal tract and that this influences regional intestinal mutation spectra and tumourigenic susceptibility. Identifying the homeostatic factors and Wnt modulators responsible for maintaining these gradients is likely to remain an area of research interest as the potential for therapeutic manipulation of Wnt in the colorectum remains a tantalising prospect.

Acknowledgements The authors thank the Animal technician staff at Cancer Research UK Clare Hall facility.

Funding This work was supported by Cancer Research UK (Clinician Scientist Fellowship to SJL) and the Wellcome Trust (CORE GRANT 090532/Z/09/Z).

Competing interests

Ethics approval All mouse work was approved by the UK Home Office and local ethics committee. Human archival tissue was obtained from St Marks Hospital, Harrow with multicentre ethics approval (MREC05/Q1606/66). Endoscopic biopsy tissue was obtained from the John Radcliffe Hospital, Oxford with local REC approval (REC 10/H0604/72).

Contributors Data acquisition by SJL, PRC, KH, AL, SS, HD, RJ and TAG. Pathology and material support by SM, MRJ, SK, SPLT, JE and SC. Study design and paper authorship by SJL and IPMT.

Provenance and peer review Not commissioned; internally peer reviewed.

Data sharing statement Unpublished data on lithium chloride stimulation of RIE cells and *Dickkopf* and *R-Spondin* Wnt modulator expression are available on request to the corresponding author.

Open access This is an open access article distributed under the terms of the Creative Commons Attribution Non-commercial, Non-Derivatives License, which permits use, distribution, and reproduction as is in any medium, provided the original work is properly cited, the work is not altered, the use is non-commercial and is otherwise in compliance with the license. See: <http://creativecommons.org/licenses/by-nc-nd/3.0/> and <http://creativecommons.org/licenses/by-nc-nd/3.0/legalcode>.

REFERENCES

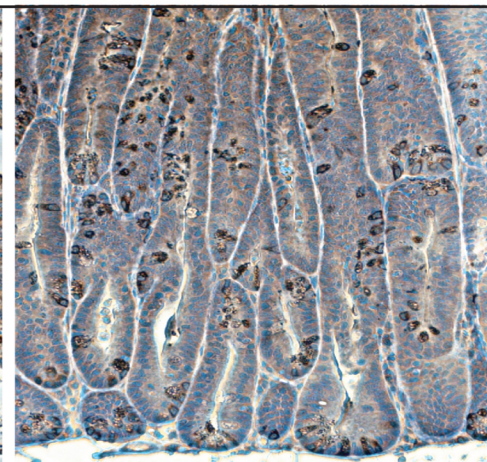
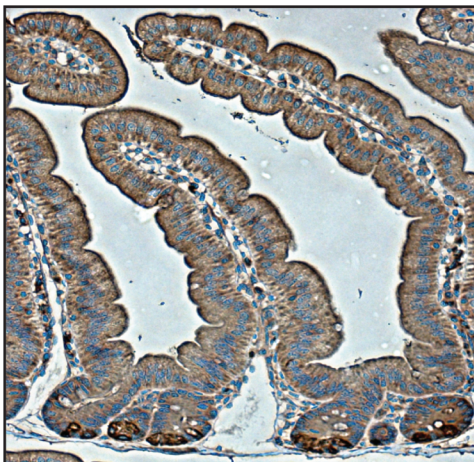
- Scoville D, Sato T, He X, *et al*. Current view: intestinal stem cells and signaling. *Gastroenterology* 2008;134:849–64.
- Kuhnert F, Davis CR, Wang HT, *et al*. Essential requirement for Wnt signaling in proliferation of adult small intestine and colon revealed by adenoviral expression of Dickkopf-1. *Proc Natl Acad Sci U S A* 2004;101:266–71.
- Radtke F, Clevers H, Riccio O. From gut homeostasis to cancer. *Curr Mol Med* 2006;6:275–89.
- Sieber OM, Tomlinson IP, Lammil H. The adenomatous polyposis coli (APC) tumor suppressor—genetics, function and disease. *Mol Med Today* 2000;6:462–9.
- Powell SM, Zilz N, Beazer-Barclay Y, *et al*. APC mutations occur early during colorectal tumorigenesis. *Nature* 1992;359:235–7.
- Miyoshi Y, Nagase H, Ando H, *et al*. Somatic mutations of the APC gene in colorectal tumors: mutation cluster region in the APC gene. *Hum Mol Genet* 1992;1:229–33.
- Lammil H, Ilyas M, Rowan A, *et al*. The type of somatic mutation at APC in familial adenomatous polyposis is determined by the site of the germline mutation: a new facet to Knudson's 'two-hit' hypothesis. *Nat Med* 1999;5:1071–5.
- Albuquerque C, Breukel C, van der Luijt R, *et al*. The 'just-right' signaling model: APC somatic mutations are selected based on a specific level of activation of the beta-catenin signaling cascade. *Hum Mol Genet* 2002;11:1549–60.
- Nagase H, Miyoshi Y, Horii A, *et al*. Correlation between the location of germline mutations in the APC gene and the number of colorectal polyps in familial adenomatous polyposis patients. *Cancer Res* 1992;52:4055–7.
- Will O, Leedham S, Elia G, *et al*. Location in the large bowel influences the APC mutations observed in FAP adenomas. *Fam Cancer* 2010;9:389–93.
- Groves CJ, Saunders BP, Spigelman AD, *et al*. Duodenal cancer in patients with familial adenomatous polyposis (FAP): results of a 10 year prospective study. *Gut* 2002;50:636–41.
- Albuquerque C, Baltazar C, Filipe B, *et al*. Colorectal cancers show distinct mutation spectra in members of the canonical WNT signaling pathway according to their anatomical location and type of genetic instability. *Genes Chromosomes Cancer* 2010;49:746–59.
- Levis A, Segditsas S, Deheragoda M, *et al*. Severe polyposis in Apc(1322T) mice is associated with submaximal Wnt signalling and increased expression of the stem cell marker Lgr5. *Gut* 2010;59:1680–6.
- Pollard P, Deheragoda M, Segditsas S, *et al*. The Apc 1322T mouse develops severe polyposis associated with submaximal nuclear beta-catenin expression. *Gastroenterology* 2009;136:2204–13.e1–13.
- Sansom OJ, Reed KR, Hayes AJ, *et al*. Loss of Apc in vivo immediately perturbs Wnt signaling, differentiation, and migration. *Genes Dev* 2004;18:1385–90.
- Fodde R, Kuipers J, Rosenberg C, *et al*. Mutations in the APC tumour suppressor gene cause chromosomal instability. *Nat Cell Biol* 2001;3:433–8.
- Harada N, Tamai Y, Ishikawa T, *et al*. Intestinal polyposis in mice with a dominant stable mutation of the beta-catenin gene. *EMBO J* 1999;18:5931–42.
- El Marjou F, Janssen K, Chang B, *et al*. Tissue-specific and inducible Cre-mediated recombination in the gut epithelium. *Genesis* 2004;39:186–93.
- Thirlwell C, Will O, Domingo E, *et al*. Clonality assessment and clonal ordering of individual neoplastic crypts shows polyclonality of colorectal adenomas. *Gastroenterology* 2010;138:1441–54.e1–7.
- Barker N, van Es J, Kuipers J, *et al*. Identification of stem cells in small intestine and colon by marker gene Lgr5. *Nature* 2007;449:1003–7.
- Stambolic V, Ruel L, Woodgett JR. Lithium inhibits glycogen synthase kinase-3 activity and mimics wingless signalling in intact cells. *Curr Biol* 1996;6:1664–8.
- Van der Flier LG, Sabates-Bellver J, Oving I, *et al*. The intestinal Wnt/TCF signature. *Gastroenterology* 2007;132:628–32.

23. **Groves C**, Lamlum H, Crabtree M, et al. Mutation cluster region, association between germline and somatic mutations and genotype-phenotype correlation in upper gastrointestinal familial adenomatous polyposis. *Am J Pathol* 2002; **160**:2055–61.
24. **Vermeulen L**, De Sousa EMF, van der Heijden M, et al. Wnt activity defines colon cancer stem cells and is regulated by the microenvironment. *Nat Cell Biol* 2010; **12**:468–76.
25. **de Lau W**, Barker N, Low TY, et al. Lgr5 homologues associate with Wnt receptors and mediate R-spondin signalling. *Nature* 2011; **476**:293–7.
26. **Ootani A**, Li X, Sangiorgi E, et al. Sustained in vitro intestinal epithelial culture within a Wnt-dependent stem cell niche. *Nat Med* 2009; **15**:701–6.
27. **Albuquerque C**, Bakker ER, van Veelen W, et al. Colorectal cancers choosing sides. *Biochim Biophys Acta* 2011; **1816**:219–31.
28. **Crosnier C**, Stamatakis D, Lewis J. Organizing cell renewal in the intestine: stem cells, signals and combinatorial control. *Nat Rev Genet* 2006; **7**:349–59.
29. **van Veelen W**, Le NH, Helvensteijn W, et al. β -catenin tyrosine 654 phosphorylation increases Wnt signalling and intestinal tumorigenesis. *Gut* 2011; **60**:1204–12.
30. **Koenders PG**, Peters WH, Wobbes T, et al. Epidermal growth factor receptor levels are lower in carcinomatous than in normal colorectal tissue. *Br J Cancer* 1992; **65**:189–92.
31. **Figueiredo JC**, Grau MV, Wallace K, et al. Global DNA hypomethylation (LINE-1) in the normal colon and lifestyle characteristics and dietary and genetic factors. *Cancer Epidemiol Biomarkers Prev* 2009; **18**:1041–9.
32. **Beishaw NJ**, Pal N, Tapp HS, et al. Patterns of DNA methylation in individual colonic crypts reveal aging and cancer-related field defects in the morphologically normal mucosa. *Carcinogenesis* 2010; **31**:1158–63.
33. **Segditsas S**, Sieber OM, Rowan A, et al. Promoter hypermethylation leads to decreased APC mRNA expression in familial polyposis and sporadic colorectal tumours, but does not substitute for truncating mutations. *Exp Mol Pathol* 2008; **85**:201–6.

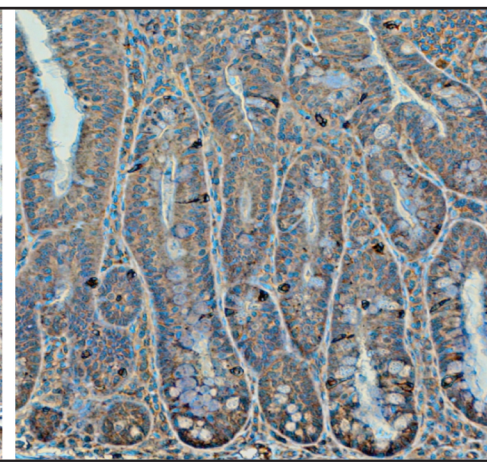
Wild-type

$Ctnnb1^{\Delta ex3}$ mice

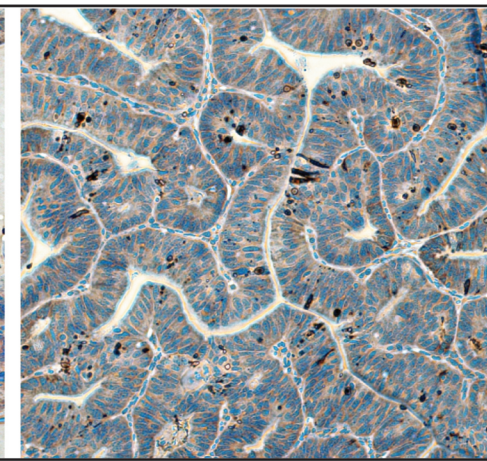
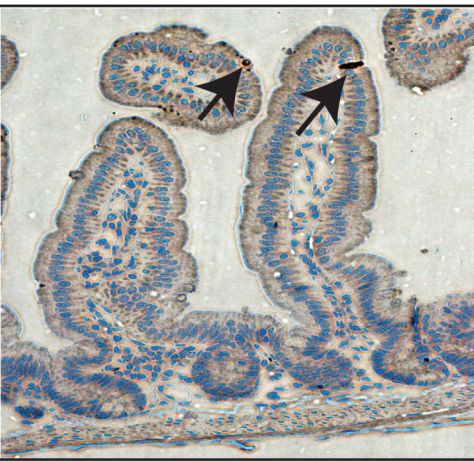
Lysozyme stain



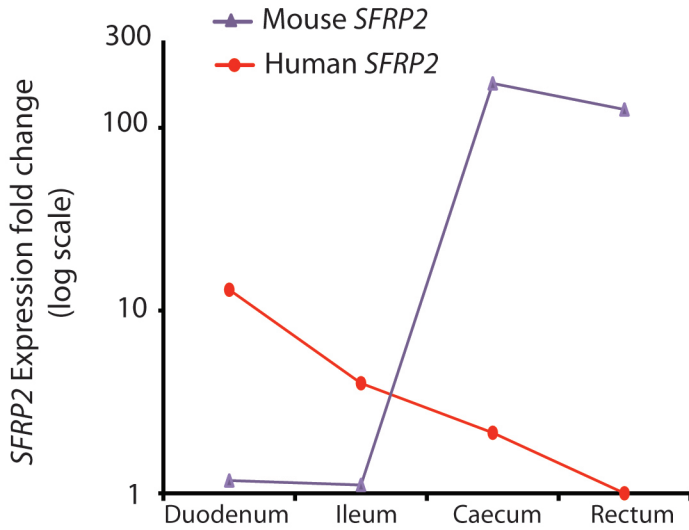
Chromogranin stain



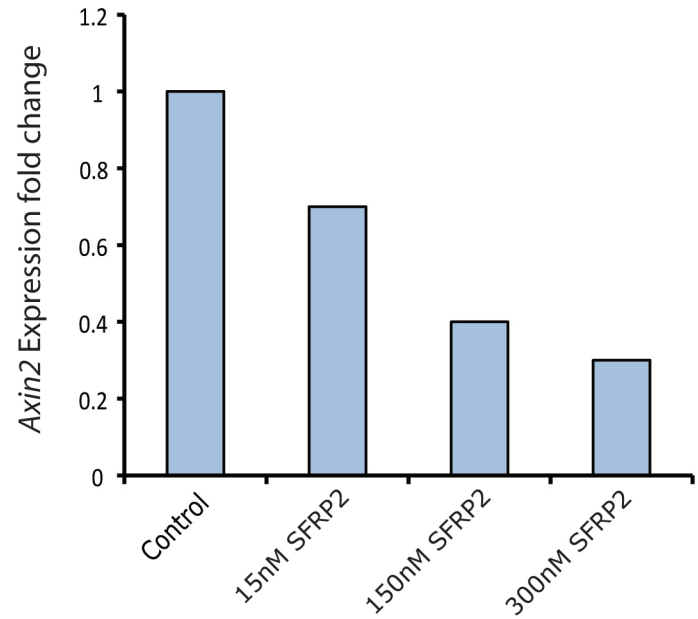
Cleaved caspase 3
stain



A.



B.



Supplementary information.

A basal gradient of Wnt and stem-cell number influences regional tumor distribution in human and mouse intestinal tracts

Supplementary Methods

Ethics and animal husbandry

All mouse work was approved by the UK Home Office and local ethics committee. Mice were housed in the barrier unit of Cancer Research UK, Clare Hall Laboratories. Human archival tissue was obtained from St Marks Hospital, Harrow with multicentre ethics approval (MREC05/Q1606/66). Endoscopic biopsy tissue was obtained from the John Radcliffe Hospital, Oxford with local REC approval (REC 10/H0604/72)

Transgenic stabilized β -catenin mouse

Animal breeding and collection of samples

Mice were genotyped for exon 3 excision using the following primers: β -catenin exon 3 forward GCTGCGTGGACAATGGCTAC, reverse GCTTTCTGTCCGGCTCCAT giving approximately 350bp fragment for mutant alleles and a 550bp fragment for wild-type alleles. Cre recombinase was detected with: forward CGGTCGATGCAACGAGTGATGAGG and reverse CCAGAGACGGAAATCCATCGCTCG primers. Intra peritoneal tamoxifen (5 consecutive days of 100 μ l of 10mg/ml tamoxifen) initiated Cre recombination in 6 week old mice, as mice of this age have undergone post-natal intestinal crypt clonal purification and are maintained on an adult diet. Mice were sacrificed at a specified time after recombination or when symptomatic (anaemic secondary to intestinal lesions or experiencing rectal prolapse). The mean time to sacrifice was 5 weeks. The intestinal tract was divided into four segments - three equal length segments of small bowel (proximal SB1, middle SB2 and distal SB3) and the colon. Each segment was flushed with phosphate buffered saline, opened longitudinally and laid out on filter paper. The samples were fixed in 10% neutral buffered formalin for 24 hours and stored in 70% ethanol. Histology samples were processed using standard methods.

Assessment of colonic Cre-mediated recombination.

Formalin fixed paraffin embedded (FFPE) colonic sections from three heterozygotes (*Ctnnb1^{ex3/+}*) and four wild-type mice were digested overnight with 30µL of Picopure™ proteinase K. TaqMan assays were designed and optimized by Applied Biosystems (Applied Biosystems, Carlsbad, Ca, USA) to the exon 3 region of the *β-catenin* gene, which is deleted in the genetically modified mice and to the exon 6 region of *ribonuclease P protein subunit p30* gene (*Rpp30*), chosen as an endogenous control following the manufacturer's recommendation. Standard curves were set up using six consecutive 2-fold dilutions of DNA extracted from a wild type mouse and were run for both *β-catenin* and *Rpp30* at all times. Colonic epithelial tissue was laser dissected away from the contaminating stroma and extracted DNA from wild-type and heterozygous mutant mice were run on the same plates and the amount of residual *β-catenin* exon 3 DNA was automatically inferred by the program from the standard curve for each gene. Values for *β-catenin* were then normalized to those for the endogenous control *Rpp30*.

Immunohistochemistry

Gut roll sections were de-waxed and rehydrated by standard methods. Endogenous peroxidase was blocked with 3% H₂O₂ in methanol for 10 minutes. Antigen retrieval was achieved by 10 minutes pressure-cooking in sodium citrate buffer at pH 6. Slides were incubated in 3% bovine serum albumin in phosphate buffered saline (PBS) for 15 minutes. Slides underwent primary antibody incubation with varying dilutions of different mouse monoclonal antibodies (Supplementary table 1). This was followed by 1:500 dilution biotinylated rabbit anti-mouse secondary antibodies (DAKO, Glostrup, Denmark) before application of a 1:500 dilution of the tertiary layer of peroxidase-conjugated streptavidin (strep-HRP: DAKO, Denmark). Each layer was applied for 45 minutes and three 5-minute PBS washes were performed between layers. Sections were then developed with 3,3-diaminobenzidine-tetrahydrochloride solution (DAB; Sigma, Gillingham, UK) for 2 minutes, followed by rinsing in tap

water and light haematoxylin counterstaining. Negative controls underwent all steps but were incubated with PBS instead of the primary antibody solution.

***In situ* hybridization**

4 μ m serial sections of formalin fixed paraffin-embedded human duodenal, ileal and colonic biopsies from 11 different patients and wild-type and transgenic mouse gut rolls were cut. Exon-spanning riboprobes were designed for human and mouse *Lgr5* and a β -*actin* probe was used for hybridization control. Riboprobes were generated by in vitro transcription using SP6 polymerase and labeled with S³⁵-UTP (human and mouse *Lgr5*) or H³-UTP (mouse *Lgr5* only) (GE Healthcare, Chalfont St Giles, UK). Other methods were as described by Poulsom *et al*.¹ In H³-UTP based assays on normal mouse intestines, the number of *Lgr5* positive cells (≥ 4 silver granules present) per crypt were counted by three different investigators (PRC, AL, SJL) on 100 crypts from each region in three different wild-type animals.

Normal mouse and human whole mount crypt analysis.

Tissue processing

Tissue was incubated in 5mls of Dulbecco's modified Eagle medium (Invitrogen) with added 30mmol/L ethylenediaminetetraacetic acid (EDTA; Sigma, UK), 0.1 mol/L dithiothreitol, and 100 μ l RNA later solution (Ambion, Austin, TX, USA) for 15 minutes. Tissue was transferred to phosphate buffered saline (PBS) and then vigorously shaken for 20 seconds. Individual intestinal crypts were then drawn up using glass pipettes and transferred to RNA lysis buffer (Qiagen, Crawley, UK). After several cycles of shaking with fresh PBS washes, complete epithelial denudement occurred and the residual mesenchymal tissue was collected and processed.

RNA extraction, reverse transcription and quantitative PCR (qRT-PCR)

RNA was extracted from individual whole mount crypts using the RNAeasy Micro kit (Qiagen, UK) which includes an on-column DNase step. Obtained RNA quality was assessed on a Bioanalyser (Agilent, Santa Clara, Ca, USA). Reverse transcription was completed straight after RNA extraction using ABI high

capacity RNA to cDNA kit (Applied Biosystems, Carlsbad, Ca, USA). Taqman Pre-Amp Mastermix (Applied Biosystems, USA) was used to pre-amplify individual crypt cDNA. The intron-spanning pre-optimized Taqman probes used, were assessed using control cDNA to ensure that no amplification bias was introduced. Quantitative RT-PCR was carried out on a 7900 Fast real-time PCR machine (Applied Biosystems, USA) using the same Taqman probes used for pre-amplification. Results were normalized to *GAPDH* and analysis was completed using the standard $\Delta\Delta Ct$ method.

Tissue culture

The rat RIE-1 small intestinal cell line was grown in RPMI medium with 10% foetal calf serum (FCS). Cells were plated out and left to grow to about 80% confluence. Following serum starvation for 24 hours, fresh serum-free medium supplemented with increasing doses of recombinant mouse Sfrp2 was added (Sfrp2 at 15nM, 150nM and 300nM concentrations). Cells were harvested after 4 hours, RNA was extracted and underwent DNase treatment and reverse transcription. qRT-PCR was then carried out for *Axin2*, an established Wnt target gene in these cells (Leedham 2010, unpublished) to assess the effect of Sfrp2 on endogenous Wnt target gene expression.

Archival human sporadic and FAP associated polyps and tumors

Tissue processing

Serial sections were cut from each block, dewaxed and carefully needle dissected using an H&E stained slide as a guide. Muscularis mucosa tissue was taken from colectomy specimens for constitutional DNA. Dissected tissue was digested overnight in 40 μ L of Picopure™ proteinase K (Arcturus Bioscience, Mt View, CA). DNA was extracted and used for *APC* sequencing and 5qLOH analysis

APC sequencing and 5qLOH analysis

DNA underwent sequencing of the mutation cluster region of *APC* using previously described primers and PCR conditions ². All samples were sequenced directly in forward and reverse orientation from a new PCR product. *APC* codons 1-1220 were also sequenced in one sample in an attempt to find mutations 5' to

the MCR. All samples underwent 5q LOH assessment using microsatellite markers D5S346, D5S421 and D5S646. Forward primers were labeled with a FAM or HEX fluorescent tag allowing identification of the two separated alleles using GENOTYPER software (Perkin-Elmer, Waltham, MASS, USA). Constitutionally homozygous markers were scored as non-informative. LOH at each marker was considered present if the area under one allelic peak in the affected crypt was less than 0.5 times or greater than 2 times that of the other allele, after normalizing the peak areas relative to constitutional DNA.

Data collection from public mutation databases (COSMIC v53)

Data were selected if both the mutation status of each *APC* allele was known (truncating mutation or LOH), and if adequate positional information to determine tumour location in the colon (right colon or left colon) was available. The number of retained 20AAR's on each mutated allele was calculated as described in the supplementary methods.

Calculation of retained 20AAR's

The total number of remaining 20AARs on the mutated allele(s) was calculated for each tumor; in cases where the tumor had two truncating *APC* mutations this was the sum of the number of 20AARs remaining on each allele; in cases where the tumor had LOH the total number of retained 20AARs was assumed to be twice the number retained on the truncated allele due to mitotic recombination.

Supplementary results

Recombinant Sfrp2 antagonises endogenous Wnt activity in RIE-1 cells.

The secreted frizzled related proteins share sequence homology with the frizzled Wnt receptor and were initially identified as secreted extracellular attenuators of Wnt, exerting their antagonistic effect by binding and sequestering Wnt proteins. In a comprehensive assessment of Sfrp action in chick neural tube cells, Sfrp2 was shown to be the most effective wnt antagonist inhibiting both endogenous and ectopic Wnt-3a induced β -catenin accumulation ³. However subsequent studies in neonatal mouse intestinal cells ⁴ kidney and salivary gland

cells⁵ demonstrated that Sfrp2 enhanced the effect of recombinant Wnt-3a promoting nuclear β -catenin accumulation and resulting in Wnt target gene expression.

We have shown that physiological *Sfrp2* expression varies considerably in the mouse intestine with colonic mesenchymal expression more than 130 fold greater than that seen in the small intestine. Furthermore this gradient is the reverse of that seen in the human (supplementary figure 1). In order to assess the effects of Sfrp2 on endogenous Wnt activity in a normal rodent intestine cell system we measured Wnt target gene expression in response to physiological and supra-physiological doses of recombinant Sfrp2. In this cell system we saw a dose dependent decrease in wnt target gene activity following incubation with recombinant Sfrp2, demonstrating that in rodent intestinal cells, Sfrp2 antagonises endogenous Wnt activity.

Supplementary table 1

Antibody	Specificity	Species	Dilution	Antigen retrieval	Source
Primary antibody					
β-catenin (610154)	Activation of Wnt pathway	Mouse	1:100	Pressure cook in sodium citrate buffer	BD Biosciences
Ki-67 (MIB1) (M7249)	S-phase marker	Rat	1:125	Pressure cook in sodium citrate buffer	DAKO
Cleaved caspase 3 (AF835)	Apoptotic cells	Rabbit	1:800	Pressure cook in sodium citrate buffer	R&D systems
Lysozyme (A0099)	Paneth cells	Rabbit	1:500	Pressure cook in sodium citrate buffer	DAKO
Chromogranin A (15160)	Enterendoctrine cells	Rabbit	1:1000	Pressure cook in sodium citrate buffer	Abcam
Secondary antibody					
IgG Biotin conjugate	Anti-mouse	Rabbit	1:300	Applied as secondary layer	DAKO
IgG Biotin Conjugate	Anti-rabbit	Goat	1:300	Applied as secondary layer	Molecular Probes

Supplementary table 1. Antibodies, dilutions and conditions.

Supplementary table 2A: Mouse whole mount crypt gene expression by qRT-PCR

Epithelial Gene/patient	SB1		SB2		SB3		Caecum		Rectum		ANOVA
	Mean (SEM) ΔCt	ΔΔCt									
<i>Ascl2</i>											
Mouse 1	5.6 (0.09)	-1.59	5.8 (0.16)	-1.39	5.7 (0.49)	-1.5	7.2 (0.17)	0	7.2 (0.36)	-0.03	p<0.001
Mouse 2	5.2 (0.26)	-3.67	6.7 (0.07)	-2.13	7.9 (0.17)	-1	8.9 (0.27)	0	7.6 (0.32)	-1.26	
Mouse 3	4.5 (0.32)	-3.18	5.9 (0.15)	-1.72	3.1 (0.54)	-2.5	7.6 (0.56)	0	6.2 (0.1)	-1.42	
Mean (SEM)	5.1 (0.35)	-2.8 (0.62)	6.16 (0.29)	-1.75 (0.21)	6.2 (0.84)	-1.7 (0.44)	7.9 (0.49)	0	7 (0.42)	-0.9 (0.44)	
<i>Lgr5</i>											
Mouse 1	6.7 (0.17)	-1.8	7.3 (0.39)	-1.2	6.5 (0.4)	-2.02	8 (0.23)	-0.54	8.5 (0.31)	0	p<0.001
Mouse 2	7.6 (0.05)	-2.2	7.3 (0.28)	-2.6	7 (0.18)	-2.86	9.8 (0.31)	0	9 (0.41)	-0.84	
Mouse 3	7.4 (0.17)	-2	8.6 (0.19)	-0.7	6.9 (0.4)	-2.47	9.4(0.64)	0	8.3 (0.23)	-1.04	
Mean (SEM)	7.23 (0.26)	-2 (0.13)	7.73 (0.45)	-1.51 (0.55)	6.79 (0.15)	-2.45 (0.24)	9.05 (0.56)	-0.18 (0.18)	8.61 (0.2)	-0.63 (0.32)	
<i>Olfm4</i>											
Mouse 1	-0.6 (0.1)	-7.39	-1 (0.25)	-7.8	-0.6(0.59)	-7.4	6.5 (0.36)	-0.29	6.8 (0.38)	0	p<0.001
Mouse 2	-0.2 (0.32)	-11.79	-0.6 (0.08)	-12.15	1 (0.27)	-10.6	11.6 (0.2)	0	9.3 (0.27)	-2.21	
Mouse 3	-0.3 (0.27)	-9.28	0.3 (0.06)	-8.7	-0.6(0.45)	-9.5	8.95 (1.12)	0	7.5 (1.45)	-1.49	
Mean (SEM)	0.08 (0.42)	-9.49 (1.27)	-0.44 (0.37)	-9.54 (1.33)	-0.66 (0.58)	-9.15 (0.9)	11.46 (1.54)	-0.1 (0.1)	7.87 (0.76)	-1.23 (0.65)	
<i>Sox4</i>											
Mouse 1	9.1 (0.01)	-2.9	10.1 (0.27)	-1.9	10.0 (0.39)	-2	11.6 (0.2)	-0.4	12.0 (0.2)	0	p<0.001
Mouse 2	9.9 (0.02)	-2.8	10.6 (0.22)	-2.1	10.6 (0.21)	-2	12.6 (0.4)	0	11.6 (0.3)	-1	
Mouse 3	9.2 (0.32)	-3.3	11 (0.21)	-1.6	10.3 (0.28)	-2.2	12.5 (0.3)	0	10.7 (0.2)	-1.9	
Mean (SEM)	9.4 (0.24)	-2.99 (0.18)	10.55 (0.25)	-1.84 (0.16)	10.3 (0.17)	-2.09 (0.07)	12.26 (0.33)	-0.13 (0.13)	11.43 (0.39)	-0.97 (0.53)	
<i>Bmp2</i>											
Mouse 1	9.2 (0.32)	0	9.2 (0.09)	-0.1	7.3 (0.1)	-1.9	7.5 (0.2)	-1.7	6.3 (0.5)	-2.9	p<0.001
Mouse 2	8.8 (0.11)	0	8.6 (0.22)	-0.3	7.2 (0.22)	-1.6	8.5 (0.6)	-0.3	5.7 (0.2)	-3.1	
Mouse 3	10.3 (0.27)	0	9.7 (0.41)	-0.6	8 (0.62)	-2.2	7.2 (0.4)	-3.1	5.9 (0.3)	-4.4	
Mean (SEM)	9.44 (0.43)	0	9.14 (0.32)	-0.3 (0.15)	9.01 (0.34)	-1.9 (0.17)	7.71 (0.4)	-1.73 (0.8)	5.96 (0.16)	3.48 (0.45)	
<i>Axin2</i>											
Mouse 1	4.05 (0.04)	-2.4	4.03 (0.34)	-2.4	4 (0.28)	-2.5	6.2 (0.28)	-0.31	6.47 (0.1)	0	p<0.001
Mouse 2	4.32 (0.09)	-3.1	4.5 (0.24)	-2.9	4.3 (0.14)	-3.1	7.4 (0.19)	0	5.79 (0.2)	-1.6	
Mouse 3	3.73 (0.42)	-4.3	4 (0.3)	-4	4.3 (0.34)	-3.8	8.1 (0.1)	0	6.37 (0.55)	-1.7	
Mean (SEM)	4.03 (0.17)	-3.28 (0.56)	4.19 (0.15)	-3.13 (0.47)	4.18 (0.09)	-3.14 (0.37)	7.21 (0.34)	-0.1 (0.1)	6.21 (0.21)	-1.1 (0.55)	
<i>Ccnd1</i>											
Mouse 1	4.8 (0.13)	-2.1	4.8 (0.25)	-2.1	4.2 (0.27)	-2.7	6.3 (0.08)	-0.6	6.9 (0.22)	0	p<0.001
Mouse 2	5.1 (0.19)	-1.6	4.15 (0.19)	-2.5	3.7 (0.18)	-3	6.7 (0.21)	0	5.7 (0.07)	-1	
Mouse 3	4.95 (0.33)	-2.4	5.8 (0.14)	-1.5	3.9 (0.22)	-3.9	7.3 (0.44)	0	6.4 (0.19)	-0.9	
Mean (SEM)	4.96 (0.08)	-2.02 (0.25)	4.93 (0.48)	-2.05 (0.29)	3.78 (0.24)	-3.2 (0.37)	6.78 (0.29)	-0.2 (0.2)	6.33 (0.37)	-0.65 (0.32)	

<i>EphB2</i>											
Mouse 1	4.8 (0.16)	-0.5	4.8 (0.25)	-0.5	4.3 (0.3)	-1	4.5 (0.2)	-0.82	5.3 (0.14)	0	p=0.1
Mouse 2	2 (0.89)	-3.7	4.1 (0.25)	-1.6	4.1 (0.15)	-1.56	5.7 (0.4)	0	5.1 (0.31)	-0.56	
Mouse 3	4.5 (0.24)	-1.85	5.3 (0.13)	-1	4.6 (0.42)	-1.8	6.3 (0.02)	0	5.15 (0.20)	-1.2	
Mean (SEM)	3.75 (0.88)	-2.02 (0.91)	4.74 (0.37)	-1.03 (0.34)	4.33 (0.12)	-1.44 (0.23)	5.49 (0.54)	-0.27 (0.27)	5.19 (0.06)	-0.58 (0.33)	
<i>Lef1</i>											
Mouse 1	11.8 (0.23)	-1.2	12.1(2)	-0.9	12.6 (0.28)	-0.4	13 (0.34)	0	12.8 (1.2)	-0.2	
Mouse 2	14.4 (1.12)	-0.4	13.2 (0.84)	-1.6	13.5 (1.09)	-1.4	14.8 (0.54)	0	14.3 (0.3)	-0.55	p=0.7
Mouse 3	12.6 (0.07)	-2.1	14.6 (0.68)	-0.1	14 (0.95)	-0.7	13.2 (1.02)	-1.5	14.7 (1.1)	0	
Mean (SEM)	12.92 (0.78)	-1.27 (0.49)	13.29 (0.72)	-0.9 (0.43)	13.36 (0.41)	-0.82 (0.28)	13.68 (0.59)	-0.51 (0.51)	13.94 (0.58)	-0.25 (0.16)	
<i>EphB3</i>											
Mouse 1	8.7 (0.17)	-1	8.1 (0.4)	-1.6	7.8 (0.3)	-1.9	9.7 (0.27)	0	8.4 (0.1)	-1.3	
Mouse 2	7.4(0.13)	-1.9	7.9 (0.2)	-1.3	7.8 (0.31)	-1.4	9.2 (0.35)	0	7.6 (0.2)	-1.6	p=0.1
Mouse 3	5.7 (0.14)	-4.3	9.8 (0.23)	-0.1	8.4 (0.43)	-1.6	10 (0.35)	0	8.1 (0.37)	-1.8	
Mean (SEM)	7.25 (0.88)	-2.38 (0.98)	8.6 (0.62)	-1.03 (0.46)	8 (0.17)	-1.63 (0.14)	9.63 (0.22)	0	8.06 (0.23)	-1.57 (0.16)	
<i>Mmp7</i>											
Mouse 1	5.6 (0.44)	-5.9	4.4 (0.85)	-7.1	4.9 (0.31)	-6.6	11.3 (0.28)	-0.2	11.5 (0.55)	0	
Mouse 2	5.3 (0.04)	-8.9	4 (0.28)	-10.2	4.4 (0.37)	-9.8	14.14(0.79)	0	14.1 (1.13)	-0.04	p<0.001
Mouse 3	6.05 (0.52)	-8	8.3 (1.04)	-5.8	7.35 (0.15)	-6.7	14.1 (1.01)	0	12.6 (1.28)	-1.45	
Mean (SEM)	5.63 (0.23)	-7.6 (0.88)	5.5 (1.37)	-7.7 (1.3)	5.55 (0.91)	-7.68 (1.04)	13.17 (0.94)	-0.06 (0.06)	12.74 (0.76)	-0.5 (0.5)	
<i>Grem 1 (m)</i>											
Mouse 1	4.8	-1.1	5.7	0	2.5	-3.2	4.3	-1.4	5.0	0.7	
Mouse 2	7.3	0	4.5	-2.8	3.3	-4	4.7	-2.6	3.2	-4.1	p=0.36
Mouse 3	4.4	-1	5.4	0	5	-0.4	3.8	-1.6	4.9	-0.5	
Mean (SEM)	5.5 (0.9)	0.7 (0.35)	5.2 (0.4)	0.93 (0.9)	3.6 (0.7)	-2.53 (1.1)	4.3 (0.3)	-1.86 (0.4)	4.4 (0.6)	-1.3 (1.44)	
<i>Grem 2 (m)</i>											
Mouse 1	7.0	0	6.0	-1	5.6	-1.4	3.1	-3.9	5.6	-1.4	
Mouse 2	11.0	0	7.1	-3.9	7.1	-3.9	3.6	-7.4	5.4	-5.6	p=0.05
Mouse 3	7.8	0	7.6	-0.2	6.5	-1.3	3.6	-4.2	7.4	-0.4	
Mean (SEM)	8.6 (1.2)	0	6.9 (0.5)	-1.7 (1.1)	6.4 (0.4)	-2.2 (0.85)	3.4 (0.2)	-5.2 (1.12)	6.1 (0.6)	-2.5 (1.6)	
<i>Hgf (m)</i>											
Mouse 1	8.0	-1.9	7.4	-2.5	8.4	-1.5	8.4	-1.5	9.9	0	
Mouse 2	7.8	-2	8.4	-1.5	9.8	0	8.9	-0.9	9.7	-0.1	p=0.04
Mouse 3	8.2	-3.4	8.7	-2.9	9	-2.6	8.6	-3	11.6	0	
Mean (SEM)	8 (0.1)	-2.4 (0.5)	8.2 (0.4)	-2.3 (1.7)	9.1 (0.4)	-1.36 (0.75)	8.6 (0.1)	-1.8 (0.6)	10.4 (0.6)	-0.03 (0.03)	
<i>Sfrp2 (m)</i>											
Mouse 1	13.7	0	13.7	0	11.8	-1.9	7.4	-6.3	6.9	-6.8	
Mouse 2	15.6	0	12.3	-3.3	14.3	-1.3	8.6	-7	5.9	-9.7	p=0.035
Mouse 3	10.8	4.9	15.7	-4.9	14.3	-1.4	2.5	-13.2	7.1	-8.	
Mean (SEM)	13.4 (1.4)	-1.63 (1.6)	15.6 (2.6)	-2.7 (1.4)	13.5 (0.8)	-1.5 (0.18)	6.2 (1.9)	-8.8 (2.2)	6.6 (0.4)	-8.4 (0.8)	

Supplementary table 2B: Human whole mount crypt gene expression by qRT-PCR

Epithelial Gene/patient	Duodenum		Ileum		Caecum		Rectum		ANOVA
	Mean (SEM) ΔCt	ΔΔCt	Mean (SEM) ΔCt	ΔΔCt	Mean (SEM) ΔCt	ΔΔCt	Mean (SEM) ΔCt	ΔΔCt	
LGR5									p<0.001
Patient 1	6.7 (0.64)	-2.4	5.5 (0.27)	-3.6	6.2 (0.61)	-3	9.1 (1.1)	0	
Patient 2	7.5 (0.74)	-0.8	5.3 (0.95)	-3	7.7 (0.46)	-0.56	8.3 (0.2)	0	
Patient 3	9 (0.55)	-1.4	5.5 (0.38)	-3.9	9.4 (0.21)	0	9.4 (0.2)	0	
Patient 4	6.6 (0.23)	-2.3	6.2 (0.22)	-2.7	7.8 (0.25)	-1.1	8.9 (0.4)	0	
OLFM4									
Patient 1	-2 (0.5)	-4.5	-4.1 (0.23)	-6.6	1.6 (0.6)	-0.9	2.5 (1.5)	0	p<0.001
Patient 2	-2.1(0.2)	-3.9	-2.1 (0.37)	-3.9	-1.9 (0.4)	-3.6	1.8 (1.16)	0	
Patient 3	0.01 (0.2)	-4	-1.8 (0.33)	-5.8	-0.6 (0.8)	-4.6	4 (0.3)	0	
Patient 4	-1 (0.6)	-6.6	-1.9 (0.1)	-7.5	-0.6 (0.4)	-6.2	5.5 (0.25)	0	
Mean (SEM)	-1.29 (0.5)	-4.8 (0.62)	-2.5 (0.55)	-5.94 (0.77)	-0.37 (0.73)	-3.83 (1.11)	3.46 (0.84)	0	
BMP2									p<0.001
Patient 1	7.8 (0.2)	0	7.6 (0.2)	-0.14	5 (0.6)	-2.8	4.8 (0.1)	-3	
Patient 2	6.5 (0.7)	-0.9	7.3 (0.4)	0	5.3 (0.3)	-2	4.9 (0.2)	-2.4	
Patient 3	7.9 (0.5)	-2.9	10.7(0.7)	0	6.7 (0.4)	-4	5.1 (0.1)	-5.6	
Patient 4	8.7 (0.1)	-0.3	9 (0.2)	0	8.5 (0.3)	-0.5	5.4 (0.5)	-3.6	
Mean (SEM)	7.7 (0.46)	-0.99 (0.61)	8.65 (0.76)	-0.04 (0.04)	6.39 (0.8)	-2.3 (0.74)	5.04 (0.13)	-3.65 (0.69)	
AXIN2									p=0.3
Patient 1	5.2 (0.4)	0	3.8 (0.16)	-1.4	3.9 (0.09)	-1.3	4.2 (0.2)	-0.9	
Patient 2	5.3 (0.6)	0	4.2 (0.1)	-1.1	4.6 (0.2)	-0.7	3.5 (0.34)	-1.8	
Patient 3	6.5 (0.1)	-1.74	4.5 (0.2)	-3.8	6.3 (0.4)	-2	8.3 (0.2)	0	
Patient 4	5.2 (0.2)	0	4.2 (0.3)	-1	5.2 (0.5)	-0.1	3.8 (0.5)	-1.4	
Mean (SEM)	5.56 (0.33)	-0.44 (0.44)	4.17 (0.14)	-1.8 (0.67)	4.98 (0.5)	-1.02 (0.42)	4.95 (1.12)	-1.04 (0.39)	
CCND1									p=0.8
Patient 1	4.6 (0.21)	-1.2	5.8 (0.18)	0	5.4 (0.18)	-0.37	5.6 (0.18)	-0.2	
Patient 2	4.3 (0.19)	-0.6	4.9 (0.39)	0	4.6 (0.5)	-0.34	4.6 (0.36)	-0.34	
Patient 3	5.6 (0.15)	-0.8	6.1 (0.35)	-0.35	6.4 (0.1)	0	6 (0.07)	-0.45	
Patient 4	5.3 (0.17)	-0.6	5.4 (0.19)	-0.6	6 (0.08)	0	5.9 (0.07)	-0.01	
Mean (SEM)	4.95 (0.3)	-0.81 (0.13)	5.52 (0.25)	-0.24 (0.15)	5.58 (0.39)	0.18 (0.1)	5.51 (0.32)	-0.25 (0.09)	
EPHB2									p=0.3
Patient 1	1.7 (0.4)	-1.1	1.2 (0.2)	-1.6	2.1 (0.3)	-0.7	2.8 (0.5)	0	
Patient 2	1.4 (0.3)	-1.2	1.3 (0.01)	-1.2	1.8 (0.2)	-0.7	2.5 (0.2)	0	
Patient 3	3.5 (0.2)	-1	2 (0.1)	-2.5	3.5 (0.2)	-1	4.5 (0.04)	0	
Patient 4	3.2 (0.44)	-0.7	2.4 (0.1)	-1.5	2.7 (0.3)	-1.1	3.8(0.2)	0	
Mean (SEM)	2.43 (0.52)	-0.97 (0.11)	1.74 (0.28)	-1.67 (0.28)	2.53 (0.36)	-0.88 (0.11)	3.4 (0.46)	0	

LEF1									
Patient 1	6.9 (0.42)	-7.4	8.8 (0.4)	-5.6	10.3 (0.5)	-4	14.3 (1.3)	0	p<0.01
Patient 2	9.2 (0.37)	-3	9 (0.6)	-3.2	12.2 (0.6)	0	12.1 (0.3)	-0.1	
Patient 3	8.9 (0.36)	-3.5	7.6 (0.3)	-4.8	11.8 (0.6)	-0.5	12.4 (0.3)	0	
Patient 4	7.4 (0.76)	-3.1	7.5 (0.2)	-3	9.7 (0.4)	-0.8	10.5 (0.4)	0	
Mean (SEM)	8.1 (0.55)	-4.24 (1.04)	8.2 (0.39)	-4.13 (0.62)	11.01 (0.6)	-1.32 (0.92)	12.31 (0.78)	-0.02 (0.02)	
EPHB3									
Patient 1	12.9 (0.59)	-0.54	11.7 (0.19)	-1.7	10 (0.26)	-3.3	13.4 (0.92)	0	p=0.05
Patient 2	14.8 (0.27)	0	10 (0.65)	-4.8	14.5 (0.62)	-0.3	14 (0.16)	-0.8	
Patient 3	16 (0.22)	0	13.4 (0.55)	-2.5	14.8 (0.22)	-1.1	14.4 (0.15)	-1.6	
Patient 4	12.6 (0.55)	-2.22	12 (0.74)	-2.8	14.4 (0.49)	-0.4	14.8 (0.18)	0	
Mean (SEM)	14.05 (0.8)	-0.69 (0.52)	11.78 (0.71)	-2.96 (0.66)	13.47 (1.13)	-1.27 (0.7)	14.15 (0.3)	-0.59 (0.38)	
GREM1									
Patient 1	8	-0.3	7.5	-0.8	7.3	-1	8.3	0	p=0.7
Patient 2	7.4	-0.3	7.1	-0.6	6.5	-1.2	7.7	0	
Patient 3	8.6	-1.3	8.9	-1	9.9	0	9.8	-0.1	
Patient 4	8.2	-2.2	8.3	-2.1	10.4	0	9.9	-0.5	
Mean (SEM)	8.05 (0.25)	-1.03 (0.46)	7.95 (0.4)	1.13 (0.34)	8.53 (0.96)	-0.55 (0.3)	8.9 (0.54)	-0.15 (0.1)	
GREM2									
Patient 1	6.8	-1.1	7.9	0	6	-1.9	6.9	-1	p=0.2
Patient 2	6.4	-2.2	5.3	-3.3	7.3	-1.3	8.6	0	
Patient 3	6	-3.1	6.8	-2.3	7.7	-1.4	9.1	0	
Patient 4	fail	fail	fail	fail	fail	fail	fail	fail	
Mean (SEM)	6.4 (0.2)	-2.1 (0.5)	6.7 (0.65)	-1.9 (0.8)	7 (0.4)	-1.5 (0.16)	8.2 (0.6)	-0.3 (0.3)	
HGF									
Patient 1	5.9	-4.5	6.4	-4	7.1	-3.3	10.4	0	p=0.05
Patient 2	6.4	-2.2	8.6	0	6.2	-2.4	8.5	-0.1	
Patient 3	5.8	-3.4	6	-3.2	5	-4.2	9.2	0	
Patient 4	6	-2.6	5.8	-2.8	5.5	-3.1	8.6	0	
Mean (SEM)	6 (0.16)	-3.4 (0.6)	7 (0.7)	-2.4 (1.06)	6.1 (0.5)	-3.3 (0.45)	9.4 (0.5)	-0.03 (0.03)	
SFRP2									
Patient 1	4.8	-1.7	5.85	-0.65	5.4	-1.1	6.5	0	p=0.25
Patient 2	6.8	-2.4	9.6	0	9.4	-0.2	9.2	-0.4	
Patient 3	7.6	-4.2	8.4	-3.4	10.6	-1.2	11.8	0	
Patient 4	7.8	-4.9	8.7	-4	10.6	-2.1	12.7	0	
Mean (SEM)	6.4 (0.7)	-2.7 (0.6)	7.95 (0.95)	-1.35 (0.9)	8.5 (1.4)	-0.8 (0.3)	9.2 (1.3)	0.13 (0.1)	

Supplementary tables 2A and B.

qRT-PCR gene expression data for mouse (supplementary table 2A) and human (supplementary table 2B) whole mount crypts and mesenchymal sections. Each patient or mouse ΔCt value was calculated from the ΔCt values of 4-5 individual crypts or from a single denuded mesenchymal section, for each gene from each region. Mesenchymal genes are indicated by (m). For calculation of $\Delta\Delta Ct$ values the region with the lowest gene expression was considered baseline expression for each individual mouse/patient. $\Delta\Delta Ct$ values for other regions were calculated against this baseline expression value. The mean (SEM) $\Delta\Delta Ct$ (red text) is the average of the individual mouse/patient values and was used to calculate the fold change values plotted in figure 3. ANOVA was used to calculate p values for differences in absolute gene expression between different regions.

Supplementary table 3

Patient 6 c.4630 G>T p.E1544X	Truncating	None	Unspecified colonic location							
			c.2432C>G p.S811X	c.1660C>T p.R554X	c.2432C>G p.S811X	c.694C>T p.R232X	c.994C>T, p.R332X	c.2432C>G p.S811X		
	LOH	Yes	No	No	No	No	No	No		
	Residual 20AARs	3	0	0	0	0	0	0		
Patient 7 c.8136del2 p.2711-12fs	Truncating	c.4660_61insA p.T1556fs	Rectum 1	Rectum 2	Rectum 3	Rectum 4	Rectum 5	TC 1	TC 2	TC 3
			c.4392del2 p.S1465fs	c.4660_61inA p.T1556fs	c. 4457del2 p.D1486fs	c.4392del2 p.S1465fs	c.4392del2 p.S1465fs	c.4489delC p.P1497fs	c.4489delC p.P1497fs	c.4216C>T p.Q1406X
	LOH	No	No	No	No	No	No	No	No	No
	Residual 20AARs	3	2	3	2	2	2	3	3	2
	Truncating	Colonic lesions continued...	TC 4	TC5	AC 1	AC 2	AC 3	AC 4		
			c.4318delC p.P1440fs	c.3925_29del5 p.E1309fs	c.4473delT p.A1492fs	c.4358delC p.P1453fs	c.4660_61insA p.T1556fs	c4127_28del2 p.1376fs		
	LOH		No	Yes	No	No	No	Yes		
	Residual 20 AARs		2	1, 1	2	2	3	1, 1		

Supplementary Table 3. Upper and lower GI polyp mutation profiles in individual FAP patients. Mutations are classified using standard nomenclature where c stands for complementary DNA sequence followed by the nucleotide number and the nucleotide change and p stands for protein sequence followed by the amino acid code letter change flanking the altered amino acid number. The number of retained 20 amino acid repeats (20AARs) is listed under each mutation. Significantly more 20AARs were retained in upper GI lesions than lower GI polyps (Binomial test, $p=0.002$) Fs - frame shift; DC - descending colon; TC – transverse colon; AC – ascending colon

Supplementary table 4A

Patient age, gender	Dukes stage	Location	<i>APC</i> mutation 1	<i>APC</i> mutation 2	Retained 20AARs
82 F	NK	Caecum	c.3871C>T p.Q1291X	c.645C>T p.R216X	1, 0
46 F	C	Caecum	c.3340C>T p.R1114X	c.4343delC p.T1448fs	0, 2
NK	NK	Caecum	c.847C>T p.R283X	c.4343delC p.T1448fs	0, 2
77 F	C	Caecum	c.4333insAT p.T1445fs	LOH	2, 2
77 M	NK	Ascending	c.4348C>T p.R1450X	LOH	2, 2
72 M	C	Left	c.4012C>T p.Q1338X	LOH	1, 1
81 M	B	Sigmoid	c.637C>T p.R213X	c.4231delG p.C1410fs	0, 2
71 M	A	Sigmoid	c.3943insA p.R1314fs	c.637C>T p.R213X	1, 0
73 M	B	Sigmoid	c.4659del5 p.E1554fs	c.4147insA p.M1383fs	0, 2
64 M	NK	Sigmoid	c.4334insCT p.1445fs	LOH	2, 2
86 F	B	Sigmoid	c.847C>T p.R283X	c.3949G>T p.E1317	0, 1
75 M	B	Rectum	c.3934G>T p.G1312X	LOH	1, 1
65 F	A	Rectum	c.3927del5 p.E1309fs	LOH	1, 1
56 M	B	Rectum	c.3694insC p.1232fs	LOH	0, 0
57 M	B	Rectum	c.4132C>T p.Q1378X	LOH	1, 1
83 F	C	Rectum	c.2460delT p.T820fs	LOH	0, 0
58 M	B	Rectum	c.1860delT p.L620fs	c.4308delT p.S1436fs	0, 2
75 M	NK	Rectum	c.3340C>T p.R1114X	LOH	0, 0
64 F	NK	Rectum	c.4263delT p.S1421fs	LOH	2, 2

Supplementary table 4B

COSMIC sample ID	Location	Cumulative total retained 20AAR's	COSMIC sample ID	Location	Cumulative total retained 20AAR's
736984	Right	5	1430400	Left	2
874934	Right	2	736987	Right	4
874961	Right	1	908482	Left	2
874963	Right	1	909748	Left	0
874964	Right	1	990137	Right	4
874965	Right	2	995381	Left	2
874967	Right	2	995391	Right	6
874975	Right	1	995397	Left	4
875010	Right	4	995400	Left	0
907794	Right	3	995404	Left	2
908457	Right	2	995408	Left	4
909755	Left	2	995409	Right	2
910783	Left	1	995413	Left	4
995375	Left	2	1206145	Left	4
995385	Right	5	1206183	Left	2
995387	Left	2	1235040	Right	4
995401	Right	3	1235041	Right	4
995412	Left	3	1235045	Right	2
995651	Left	3	1235046	Left	0
1231126	Left	3	1235051	Right	4
1235039	Left	2	1235054	Right	4
1235043	Right	2	1235056	Right	2
1235055	Left	1	1235058	Left	0
1235057	Left	2	1235066	Left	2
1235059	Right	2	1235067	Left	0
1235061	Right	0	1235068	Left	0
1322285	Left	1	1235069	Left	2
1322293	Right	3	1235073	Right	4
1322287	Right	2			

Supplementary table 4A and B: Sporadic colorectal cancers and cell lines

Table 4A. Genotyped sporadic colorectal cancers. 19 sporadic colorectal cancer cases from specified colonic locations were genotyped and two hits at *APC* were identified. **Table 4B. Publically available data from COSMIC v53.**

57 tumors and cell-lines with positional data and two hits at *APC* were identified. The number of retained 20 amino acid repeats (20AARs) resultant from the identified mutations is stated. Mutations are classified using standard nomenclature where “c.” stands for cDNA sequence followed by the nucleotide number and the nucleotide change and “p.” stands for protein sequence followed by the amino acid code letter change flanking the altered amino acid number.

Abbreviations M, male; F, female; LOH, loss of heterozygosity (determined by 5q microsatellite analysis); NK, not known.

Supplementary figure legends

Supplementary figure 1

Examples of immunohistochemical staining for cell lineage and apoptosis in wild-type and *Ctnnb1^{ex3}* mice.

In wild type mice lysozyme staining for Paneth cells is restricted to cells at the base of crypts. No such positional restriction is seen in the section of a *Ctnnb1^{ex3}* mouse where brown stained Paneth cells can be seen the length of the grossly enlarged crypts. Occasional chromogranin A stained cells can be seen in both normal and mutant intestinal crypts but no significant difference in number could be found. Apoptotic cells stained positive for cleaved caspase 3 (black arrows) were uncommon in the normal intestinal crypts but were significantly more prevalent in the dysplastic crypts of *Ctnnb1^{ex3}* mice.

Supplementary figure 2

A. Physiological mesenchymal *Sfrp2* expression in human and mouse intestinal tracts. Mesenchymal expression of this important Wnt modulator varies considerably along the length of the human and murine intestines, with a reverse gradient seen in the two different species. Mouse colonic mesenchymal *SFRP2* expression is greater than 130-fold that seen in the small intestinal mesenchyme.

B. Recombinant *Sfrp2* antagonises endogenous Wnt activity in rodent intestinal epithelial cells. Culturing RIE cells with recombinant SFRP2 at physiological (15nM) and supra-physiological (150 and 300nM) concentrations resulted in a dose dependent decrease in Wnt target gene activity as a consequence of endogenous physiological Wnt pathway antagonism.

Supplementary References

1. Poulsom R, Longcroft JM, Jeffery RE et al. A robust method for isotopic riboprobe in situ hybridisation to localise mRNAs in routine pathology specimens. *Eur J Histochem.* 1998;42(2):121-32.
2. Thirlwell C, Will O, Domingo E et al. Clonality assessment and clonal ordering of individual neoplastic crypts shows polyclonality of colorectal adenomas. *Gastroenterology.* 2010 Apr;138(4):1441-54, 54.e1-7.
3. Galli LM, Barnes T, Cheng T et al. Differential inhibition of Wnt-3a by Sfrp-1, Sfrp-2, and Sfrp-3. *Dev Dyn.* 2006 Mar;235(3):681-90.
4. Kress E, Rezza A, Nadjar J et al. The frizzled-related sFRP2 gene is a target of thyroid hormone receptor alpha1 and activates beta-catenin signaling in mouse intestine. *J Biol Chem.* 2009 Jan 9;284(2):1234-41.
5. von Marschall Z, Fisher LW. Secreted Frizzled-related protein-2 (sFRP2) augments canonical Wnt3a-induced signaling. *Biochem Biophys Res Commun.* 2010 Sep 24;400(3):299-304.